2-P (MIX)

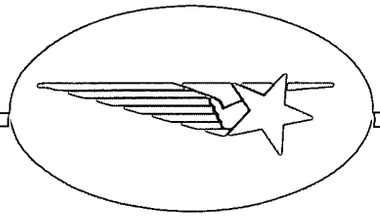

NTIS HC $5.75

(NASA-CR-130359) EXPERIMENTAL STUDY OF SPECTRAL AND SPATIAL DISTRIBUTION OF SOLAR X-RAYS Final Report (Lockheed Missiles and Space Co.) 74 p HC $5.75 CSCL 03B G3/29

N73-16793

Unclas 16575

Lockheed

MISSILES & SPACE COMPANY

A GROUP DIVISION OF LOCKHEED AIRCRAFT CORPORATION

SUNNYVALE, CALIFORNIA

FINAL REPORT

Contract NASw-1834

EXPERIMENTAL STUDY OF SPECTRAL AND SPATIAL DISTRIBUTION OF SOLAR X-RAYS

29 September 1972

Loren W. Acton

Richard C. Catura

J. Leonard Culhane

Lockheed Palo Alto Research Laboratories
3251 Hanover Street
Palo Alto, California 94304

TABLE OF CONTENTS

1. INTRODUCTION

This final report summarizes the technical results of work carried out under Contract NASw-1834 by the Space Astronomy Group of the Radiation Physics Laboratory at the Lockheed Palo Alto Research Laboratories. Two rocket flights from White Sands Missile Range (WSMR), New Mexico, were successfully completed under this program. NASA Aerobee 13.14 CS was launched at 1630 UT on 29 April 1971 and NASA Aerobee 13.15 CS was launched at 2058 UT on 24 April 1972. The scientific analysis of the flight results is being carried out under a separate contract (NAS2-6723). Results to date are included in the Appendices.

The scientific aims of the program are given in Section 2. One of the primary aims of this program was the development of improved instrumentation for solar x-ray studies. Section 3 summarizes this aspect of the work. In Section 4, we present some information gained from experience with this program and make some critical comments on needed improvements in range facilities. Some scientific results are presented in Section 5.

We especially wish to call attention to the recommendations and conclusions given in Section 6.

Dr. G. Schmidtke and Mr. W. Schweizer of the Arbeitsgruppe feur Physikalische Weltraumforschung in Freiburg, Germany, provided an additional instrument, a grazing incidence EUV grating spectrograph, for each of our two flights. The preliminary results of their work have already been published (Schweizer and Schmidtke, 1971). Our co-investigator, Dr. J.L. Culhane of University College London, provided the key elements of the position sensitive proportional counter and its pre-amplifiers for the curved crystal spectrometer test flown on Aerobee 13.15. We are gratified with the success of these international cooperations and are convinced that the cost and scientific effectiveness of our solar rocket program may be benefited by the future continuation of such arrangements.

2. SCIENTIFIC AIMS OF THE EXPERIMENTS

The objectives of the research program carried out under this contract were twofold. The primary objective was to obtain a more thorough understanding of the range of physical conditions within the solar corona; the secondary objective, to continue the development of the instrumentation and technical expertise necessary for meaningful future studies of solar x-ray emission. We are gratified that both of these objectives have been attained.

In order to attain our primary objective, we studied the line emission from the helium-like ions O VII and Ne IX. The intensity ratio of the resonance lines ($1s^2\ ^1S_o$ - $1s2p\ ^1P_1$) from these two ions provides a measure of the electron temperature of the source region. Also, according to the theory of Gabriel and Jordan (1969), the ratio of the intensity of the forbidden ($1s^2\ ^1S_o$ - $1s2s\ ^3S_1$) to the intersystem ($1s^2\ ^1S_o$ - $1s2p\ ^3P$) lines of each of these ions is sensitive to electron density. Although we had hoped to obtain a measure of the electron density of each source region, our measurements have only been able to establish an upper limit on these electron densities (see Appendices 2 and 4).

We have used the absolute intensity of the resonance line emission from source regions to determine the volume integral of the product of the electron and ion densities, the so-called emission measure of the regions. In addition, we observed the 1 to 4 A continuum in order to detect higher temperature plasma within the active regions.

For the second flight under this program (Aerobee 13.15), we modified the spectrometers to include coverage of two emission lines of Fe XVII plus the Lyman alpha line of O VIII. At the same time, the APW instrument was changed to include coverage of emission lines from Si IX, Si XI, Fe XIV and Fe XVI. The object of this increase in spectral coverage was to improve the ability to specify a realistic non-isothermal model for each active region observed.

3. INSTRUMENTATION

The instrumentation developed for the flight of Aerobee 13.14 is described in Appendices 1 and 4. In addition, the bi-monthly progress reports have described instrumental developments and modifications as they have occured for each rocket payload. For this reason, the discussion of this section will be brief.

Table 1 gives the important characteristics of the x-ray spectrometers included in the two payloads. The general layout of the payload is illustrated in Figure 1. Figure 2 is a photograph of the completed payload for Aercbee 13.14.

The bent crystal spectrometer added to the payload for the flight of Aerobee 13.15 utilized a "position sensitive" proportional counter, a detector which is able to record the position along the anode at which a pulse occurs, to measure the x-ray spectrum diffracted by the curved crystal. This sytem was flown as an engineering test of similar systems to be flown by this laboratory in 1973 as a part of the ATM-A rocket support program. Its preparation was carried out under Contract NAS2-6723 and will not be further discussed in this report except to say that the key elements of the detector and preamplifiers used were provided by Dr. J.L. Culhane of University College London, co-investigator in this program.

Figure 3 illustrates one of the technical innovations developed for this program. This large Oda-type collimator was placed in front of the crystals to define the field of view of the spectrometers. At the same time, it prevented the spectral confusion common to uncollimated Bragg spectrometers caused by multiple apparent sources at various angles to the optical axis of the instrument. The six photoetched grids were aligned on precision steel rods passing through holes of precise diameter and location which were fabricated as an integral part of each grid. The rods were supported on each end during assembly by plates with an appropriate precision hole pattern and the process of assembly was carried out on a precision flat surface plate. These collimators utilized improvements based on the experience gained by our laboratory in connection with

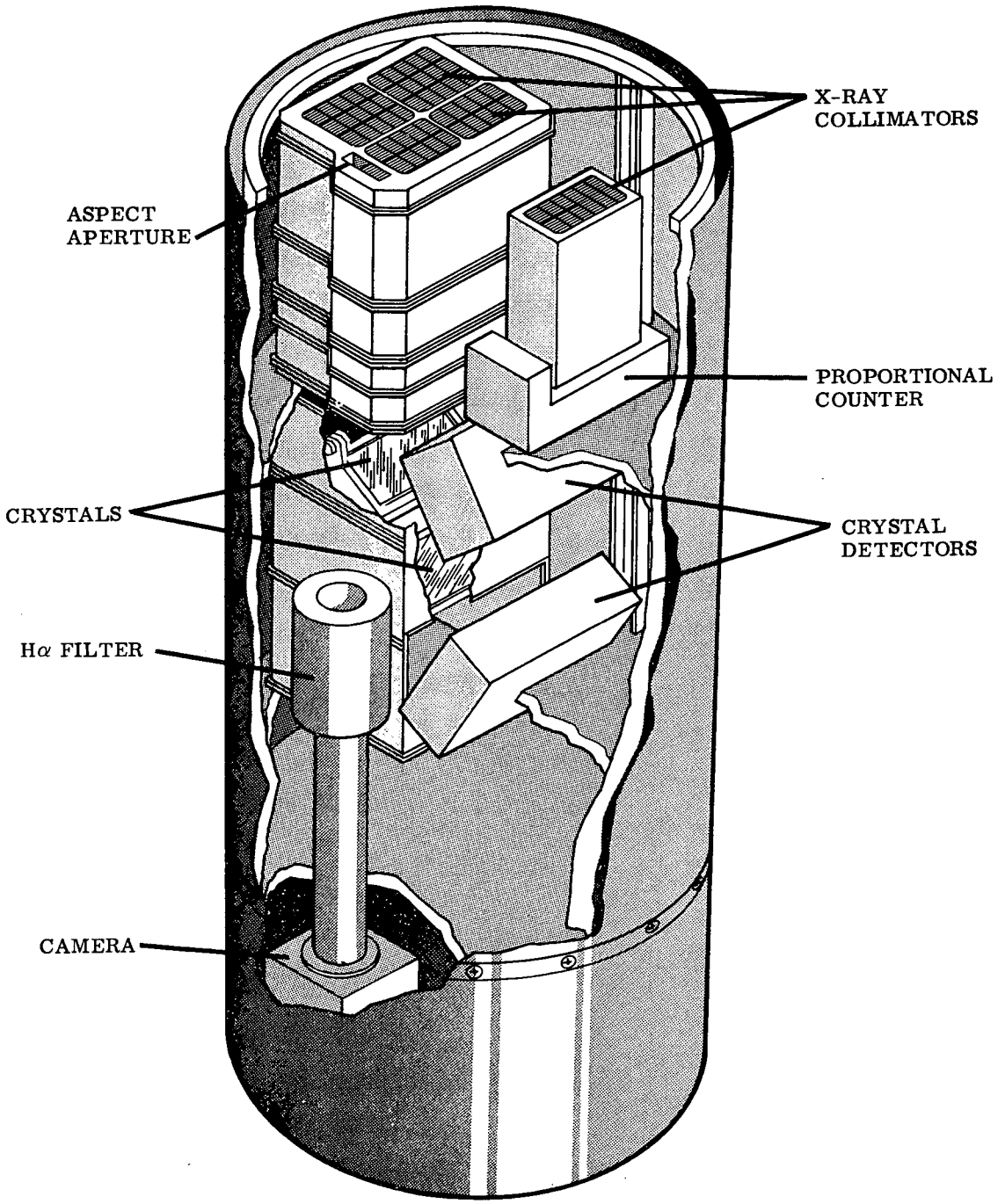

Figure 1 Artist's sketch of the rocket payload showing location of key assemblies. Light from the aspect aperture of the collimator assembly is conducted to the Hα filter by a prism which is not shown.

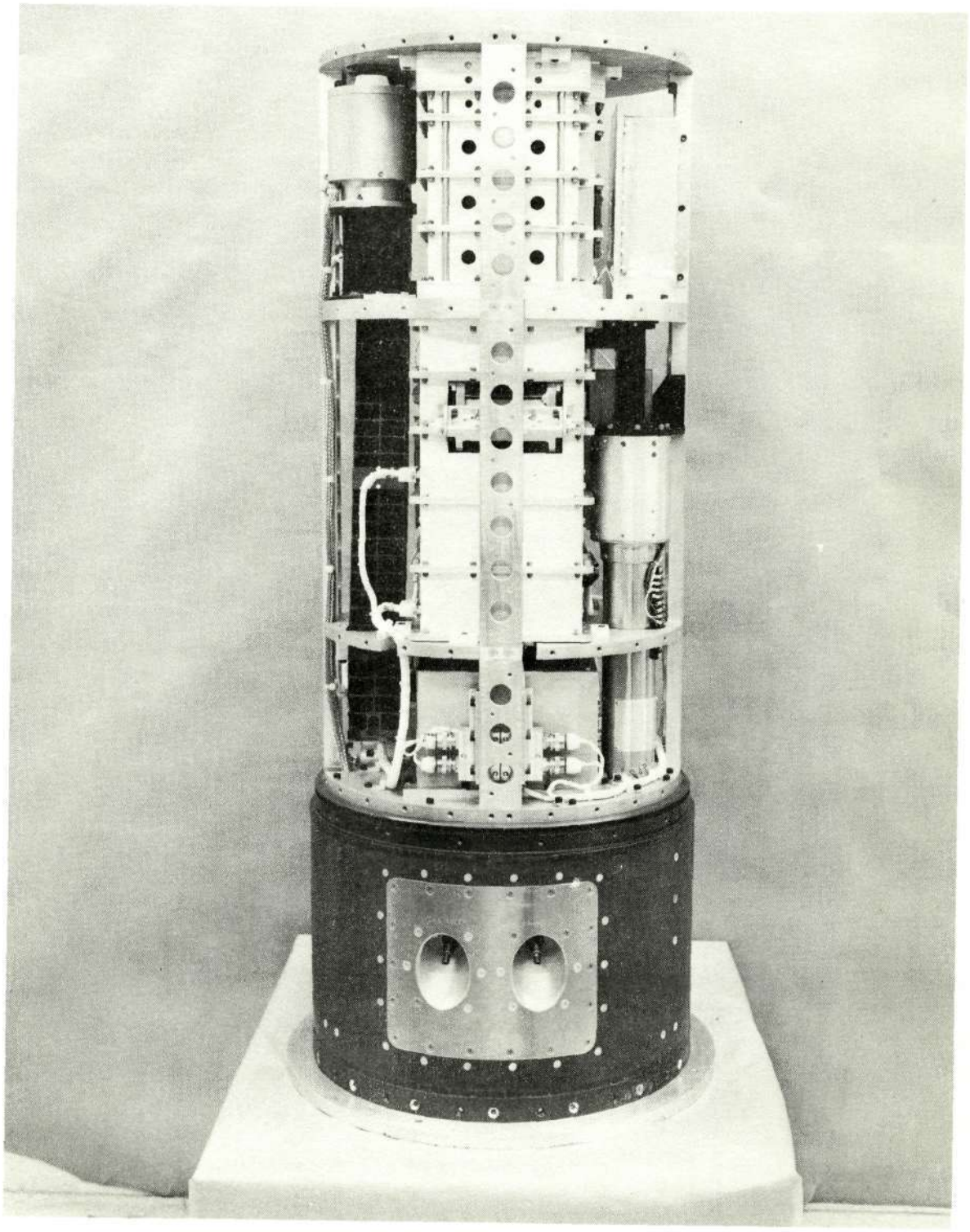

Figure 2 Side view of the assembled payload. The SPARCS fine solar sensor is on the second shelf from the top at the left. The German EUV spectrograph may be seen extending below it.

Table I

X-RAY SPECTROMETERS

System	Aerobee 13.14 λλ (A)	Aerobee 13.14 Effective Area (cm^2)	Aerobee 13.15 λλ (A)	Aerobee 13.15 Effective Area (cm^2)
Spectrometer A (Plane XTAL)	21.4-22.3	24	21.4-22.3 18.2-19.3	12 7
Collimation (FWHM)	1.7 arcmin		1.3 arcmin	
Spectrometer B (Plane XTAL)	13.3-13.8	15	13.3-13.9 14.7-15.4	7 4
Collimation (FWHM)	1.7 arcmin		1.3 arcmin	
Spectrometer C (Bent XTAL)	--		10 - 24	15
Collimation (FWHM)			3^o x 14^o	
Spectrometer D (Proportional Ctr)	0.8 - 4	12	0.8 - 4	12
Collimation (FWHM)	4.2 arcmin		4.2 arcmin	

the flight of Aerobee 4.248 under Contract NASw-1398. At that time, we successfully obtained spatially resolved observations of solar x-ray sources through the use of the first Oda-type collimator to be applied to solar studies (Catura, Acton and Fisher, 1970).

For the measurement of payload aspect, each collimator grid included a small area partially open and partially covered with a specially designed grid spacing different from that used in the x-ray portion of the collimator. Light entering this section of the collimator is passed through a 1 A optical filter centered at the hydrogen H-alpha line (6563 A) and imaged on Kodak SO-392 film in a 16mm camera which operates during the flight at a frame rate of about 4 frames per second. Light entering the open portion of this aperture forms a full disk image of the sun while light entering the grid portion of this aperture forms a diffraction pattern which is superimposed on the image of the disk. The central peak of this diffraction pattern is centered on the x-ray field of view of the collimator. Because this aspect information results from the passage of the light through the collimator itself, there is no need to maintain critical alignment between the camera system and the x-ray systems. Figure 4 is a photograph of the flight Hα telescope and camera.

The objective of the observations was to map x-ray emission from the entire disk in a single rocket flight with maximum sensitivity and spatial resolution. To accomplish this objective, the wavelength ranges of the spectrometers were restricted to narrow wavelength intervals about specific x-ray emission lines of interest. The wavelength intervals were small enough that they could be rapidly scanned by the crystals as the slit-like field of view of the spectrometers was moved across the disk. This also allowed maximum observing time for the x-ray lines of interest and permitted the x-ray detectors to remain fixed because of the narrow range of Bragg angles covered by a given spectrometer. This permitted use of large (97 cm^2 each) x-ray analyzing crystals. (See Appendix 4 for further details.)

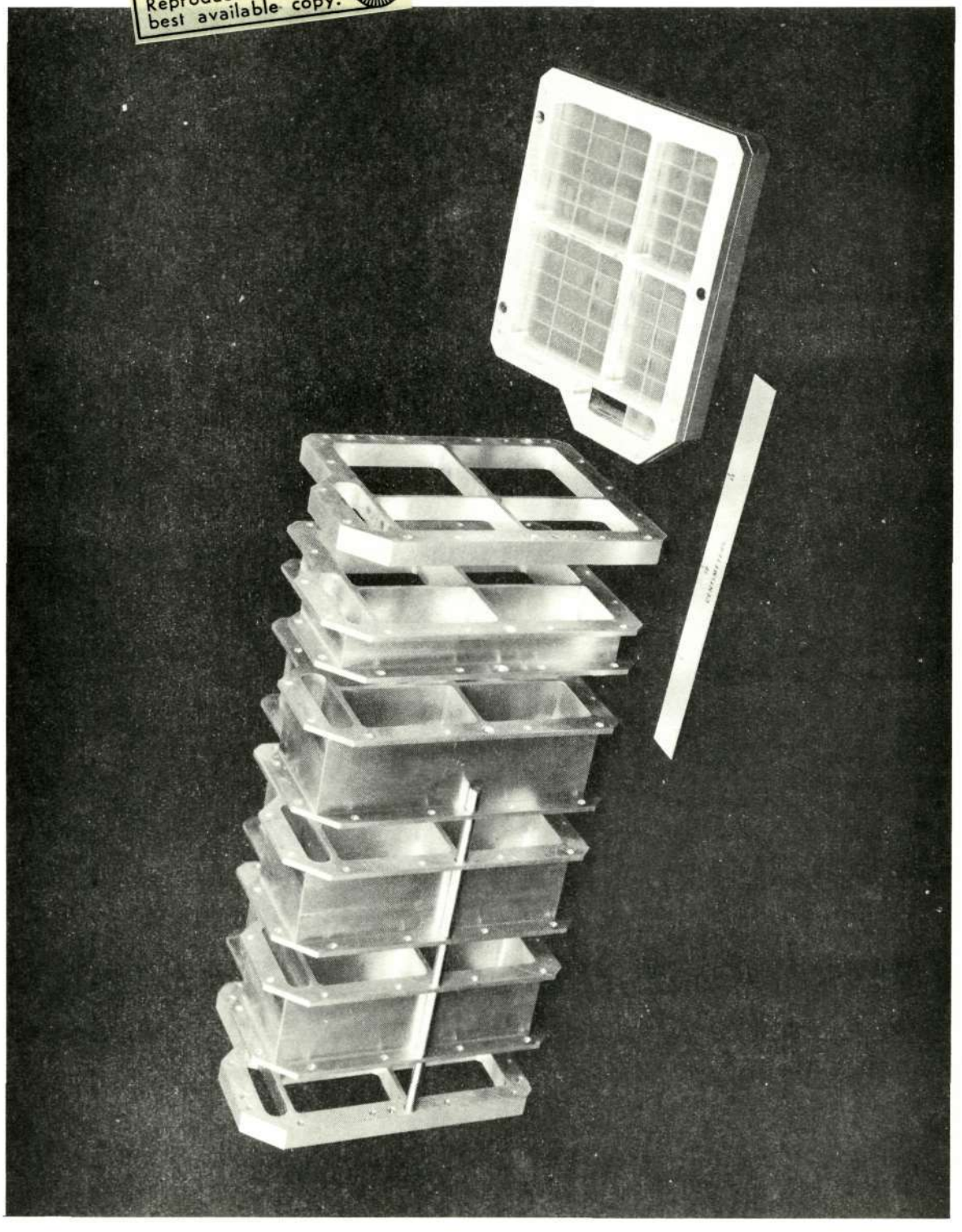

Figure 3 Exploded view of x-ray collimator assembly showing an alignment rod and one of the six collimator grids in the frame on the right.

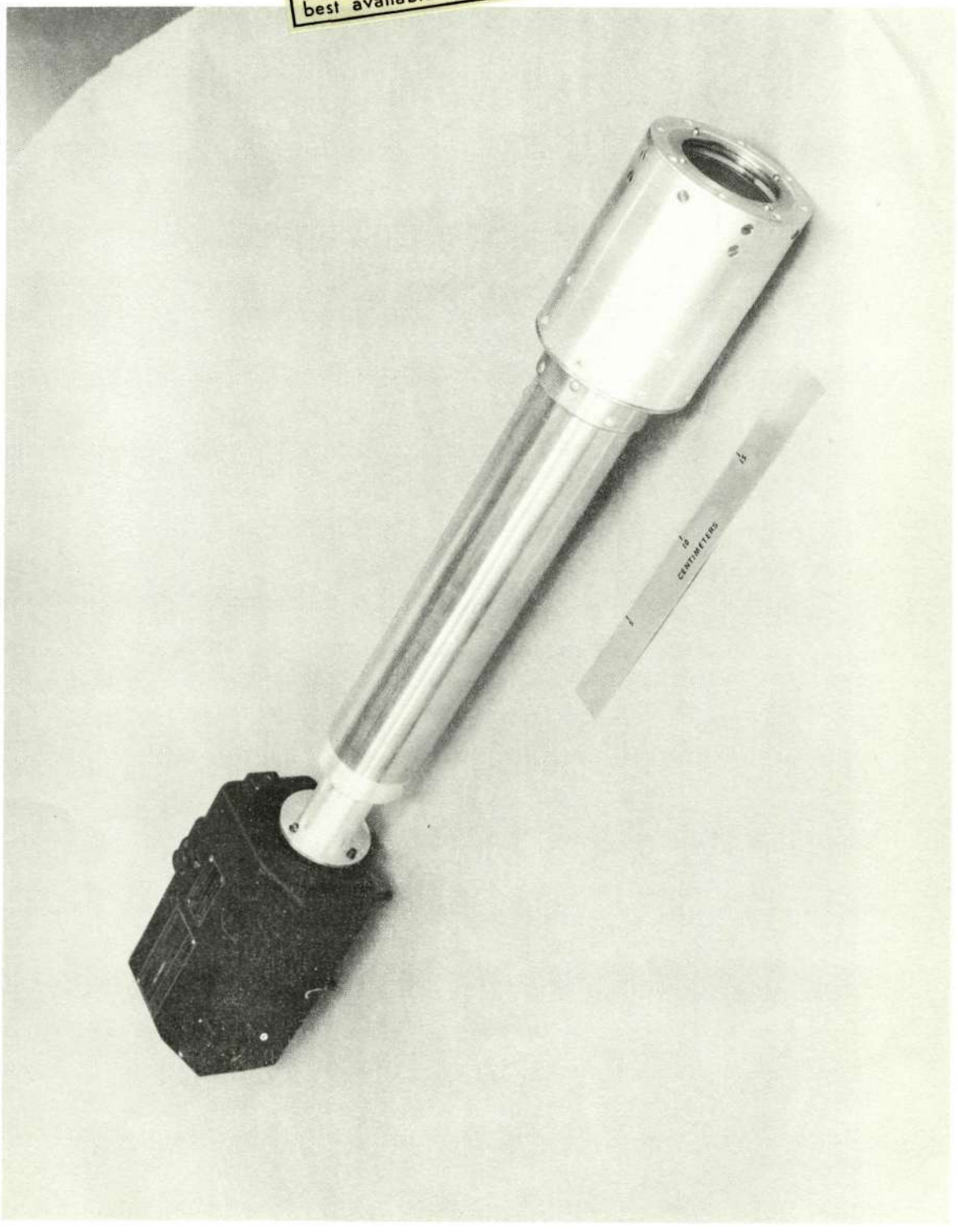

Figure 4 View of flight aspect telescope showing Hα filter housing on the right and 16mm time lapse camera on the left.

4. FLIGHT SYNOPSES

The observing plan for both flights under this contract involved payload orientation under control of the SPARCS system with the optical axis about 4 arcmin beyond the limb of the sun at a specified rocket roll angle. The optical axis and x-ray fields of view were then scanned across the sun at a specified rate of about 0.3 arcmin sec^{-1} for a distance of 40 arcmin at which time the scan was terminated. The payload was then rolled to another prescribed angle and a second scan of the disk, which occupied the remainder of the flight, was initiated. Figures 5, 6 and 7 illustrate how this observing program was performed during the flight of Aerobee 13.14. These data were obtained from the on-board Hα aspect camera. The successful execution of this complex observing program again has demonstrated the impressive capabilities of the SPARCS system.

The selection of scan directions (i.e., specification of the rocket roll angles) was done on the day of launch by direct observation of the sun with a small portable H-alpha telescope set up at the blockhouse. This system is not precise enough for work utilizing smaller fields of view. The best solution is to have high quality video or photographic images of the sun available at the WSMR launch areas either from an on-site solar telescope or transmitted in real time from a solar observatory. Sacramento Peak Observatory has an excellent solar patrol with video output and line-of-sight access to WSMR so it may be relatively easy to set up a portable microwave video link to provide this needed information to experimenters.

This program was the first program for which SPARCS was used in a scanning mode and also the first program for which NASA Ames Research Center had responsibility for instrumentation, telemetry, vehicle separation and recovery. Mr. E. Gabris and his crew at the NASA/ARC Vehicle Guidance and Control branch and their contractor, the Lockheed Missiles and Space Company, Space Systems Division, deserve warm commendation for a job well done on a complex flight program.

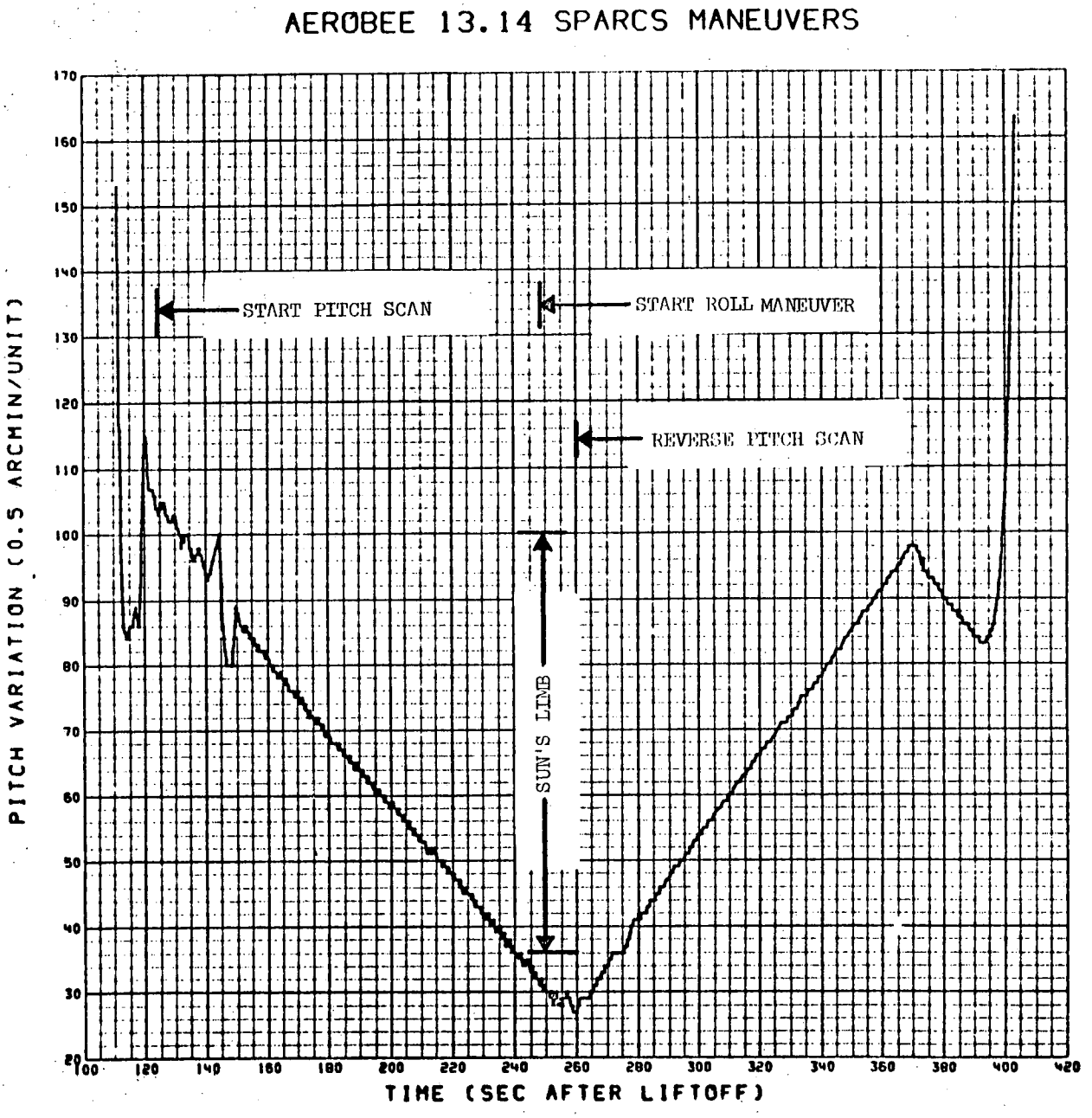

Figure 5 Motion of Aerobee 13.14 field of view in the direction of scan across solar disk.

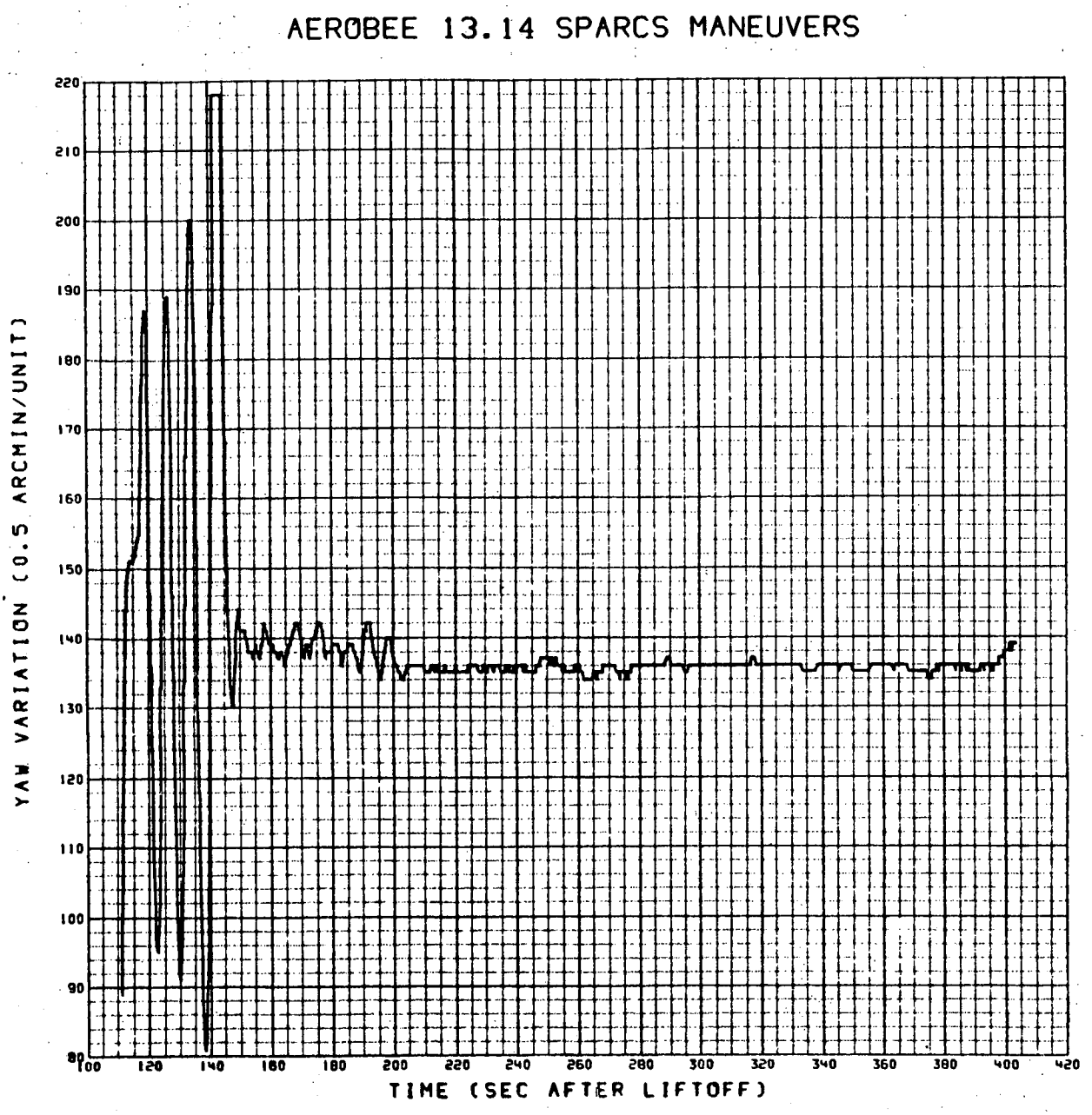

Figure 6 Motion of Aerobee 13.14 field of view in a direction perpendicular to the direction of scan.

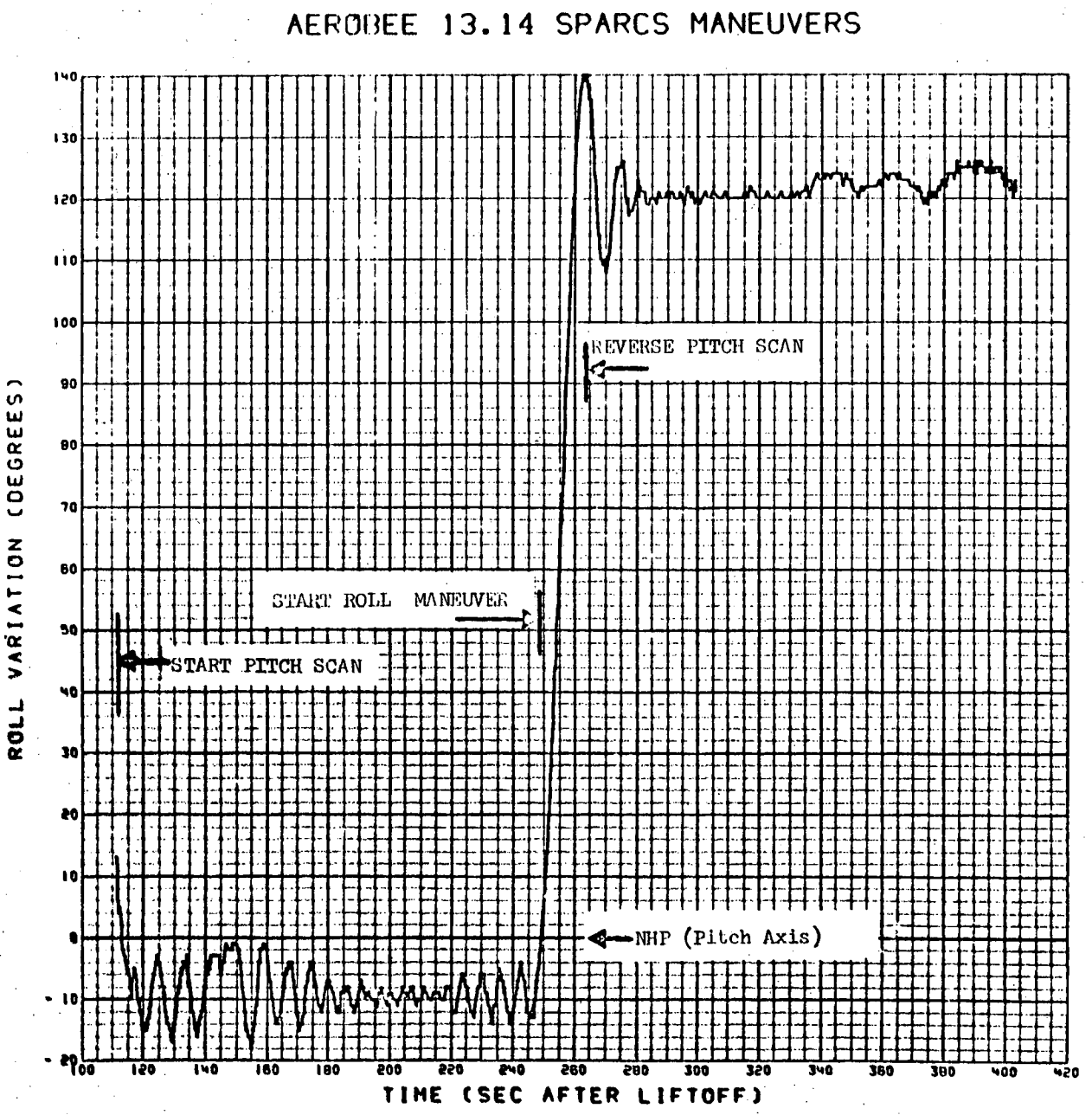

Figure 7 Motion of Aerobee 13.14 payload about the longitudinal axis.

As always, the range telemetry support of NMSU/PSL was above reproach and NASA/GSFC vehicle support left nothing to be desired. The payloads from both flights were recovered in good condition.

Telephone communications to and from the range continues to be a problem, especially for programs such as this one which attempt to coordinate supporting observations including satellite and ground based data. Connections are often poor and delayed so that critical messages do not get through. If such coordinated observational programs are to be successful, more direct and reliable access to the nation's primary telephone system must be made available to the experimenter at WSMR. This communication need will be especially critical during the upcoming ATM-A calibration and support rocket flights.

We experienced a difficulty with the thin-window proportional counters used in the spectrometers which we mention here since the information may be useful to other experimenters. Because of limited space, it was necessary to design these detectors without the evacuated antechambers which are sometimes used to protect the thin windows from rapid changes in differential pressure across the window. In order to minimize the differential pressure across the thin (approximately 2 micrometers) polypropylene windows the detectors were operated at about 0.5 atmosphere pressure. Supporting grids were provided both inside and outside of the window. This design minimized differential pressure across the thin window but resulted in changes in the direction of the differential pressure across the window from inward to outward in flight and to some extent during counter operation in laboratory testing. After a few cycles of changes in the direction of differential pressure across the window, the thin windows usually developed leaks. We now believe that a better design for thin window detectors without antechambers should involve operating them slightly above atmospheric pressure. In this way, the differential pressure across the window is always in the same direction. The films themselves are strong enough to support the higher pressure and the windows do not undergo cycling of the differential pressure which we feel shortens their useful life. Laboratory tests have supported this conclusion.

An overstressed part in the mechanical-pyrotechnic apparatus which served to release the crystal spectrometers failed on one of the Aerobee 13.15 spectrometers and the crystal remained pinned on the Ne IX resonance line throughout the flight. This resulted in improved spatial information because of better counting statistics but at the loss of the spectrum scan in the Ne IX and Fe XVII regions. Further designs will be modified based on this experience.

5. RESULTS

The scientific results from this program have been gratifying. Although this contract did not include funds for scientific data analysis, this work is being carried out under Contract NAS2-6723 and the six publications which have so far resulted from the Aerobee 13.14 data are included in the Appendices. We feel that the interpretation of the data based on a non-isothermal source model (see Appendices 4 and 5) is a distinct improvement toward the understanding of the coronal volumes responsible for this emission. We anxiously await improved observations of more emission lines so that this type of analysis may be carried further.

The reduction and analysis of the data from the flight of Aerobee 13.15 is underway and only preliminary results are available. Figures 8 and 9 show the spatial distribution of Ne IX emission as measured on the first and second scans of the disk and the O VII emission from the second (pole to pole) scan. Figure 10 compares the temperature distribution in the corona derived from the West to East scan of Aerobee 13.14 to the pole to pole distribution from the Aerobee 13.15 data. These results include the assumption that the O VII and Ne IX emissions are from the same isothermal volume within a given field of view. Data from Aerobee 13.15 have been normalized to the 13.14 data at the low temperature, quiet corona, regions.

6. SUMMARY AND RECOMMENDATIONS

The technique of using large-area collimated Bragg spectrometers scanning narrow wavelength intervals to achieve the sensitivity necessary for solar coronal surveys from rockets has been well proven under this contract. Also, the basic capability of the SPARCS pointing control for

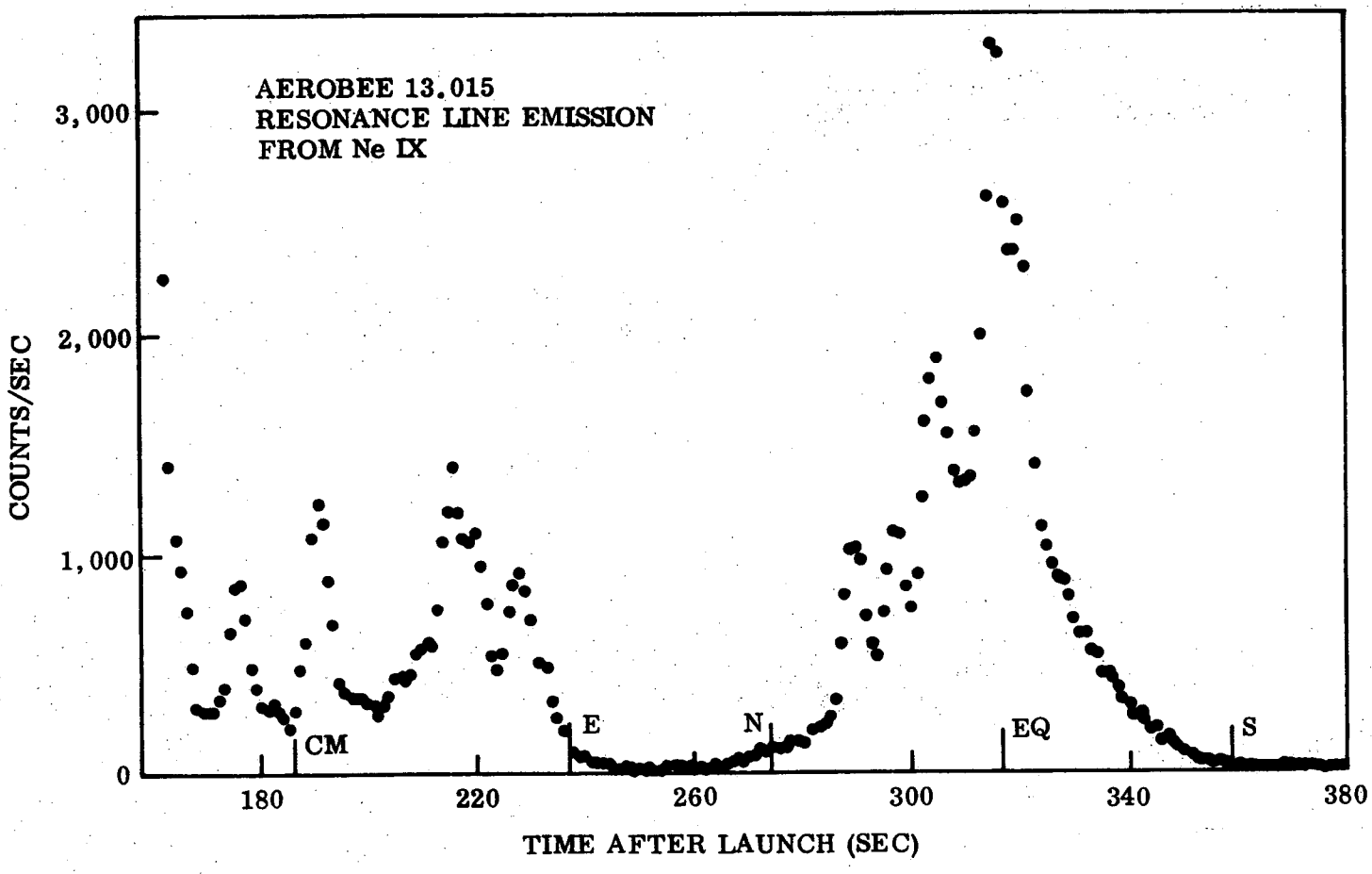

Figure 8 Distribution of Ne IX emission as measured in a W-E and a N-S scan. Data before 160 sec missing because of pointing instability. Rocket roll maneuver occurred around 260 sec. CM means central meridian and EQ means solar equator.

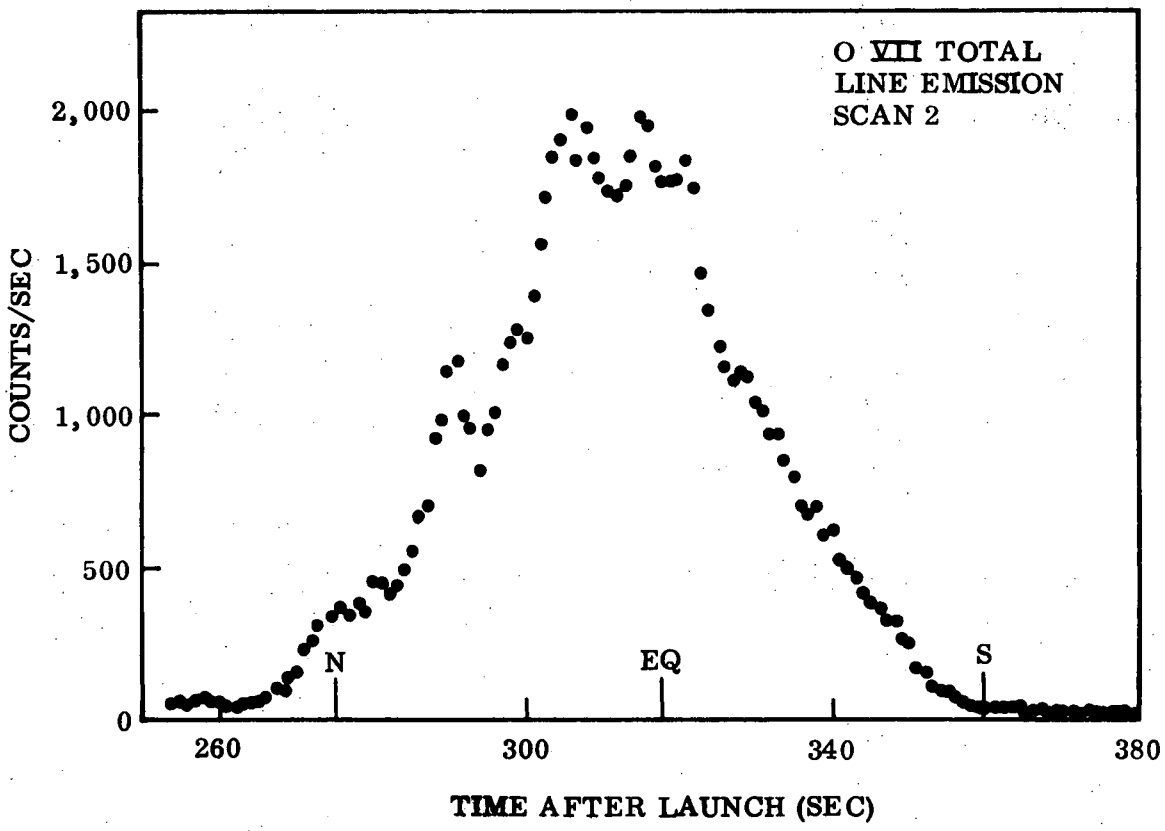

Figure 9 Pole to pole distribution of O VII emission. Compare to RH portion of Figure 8.

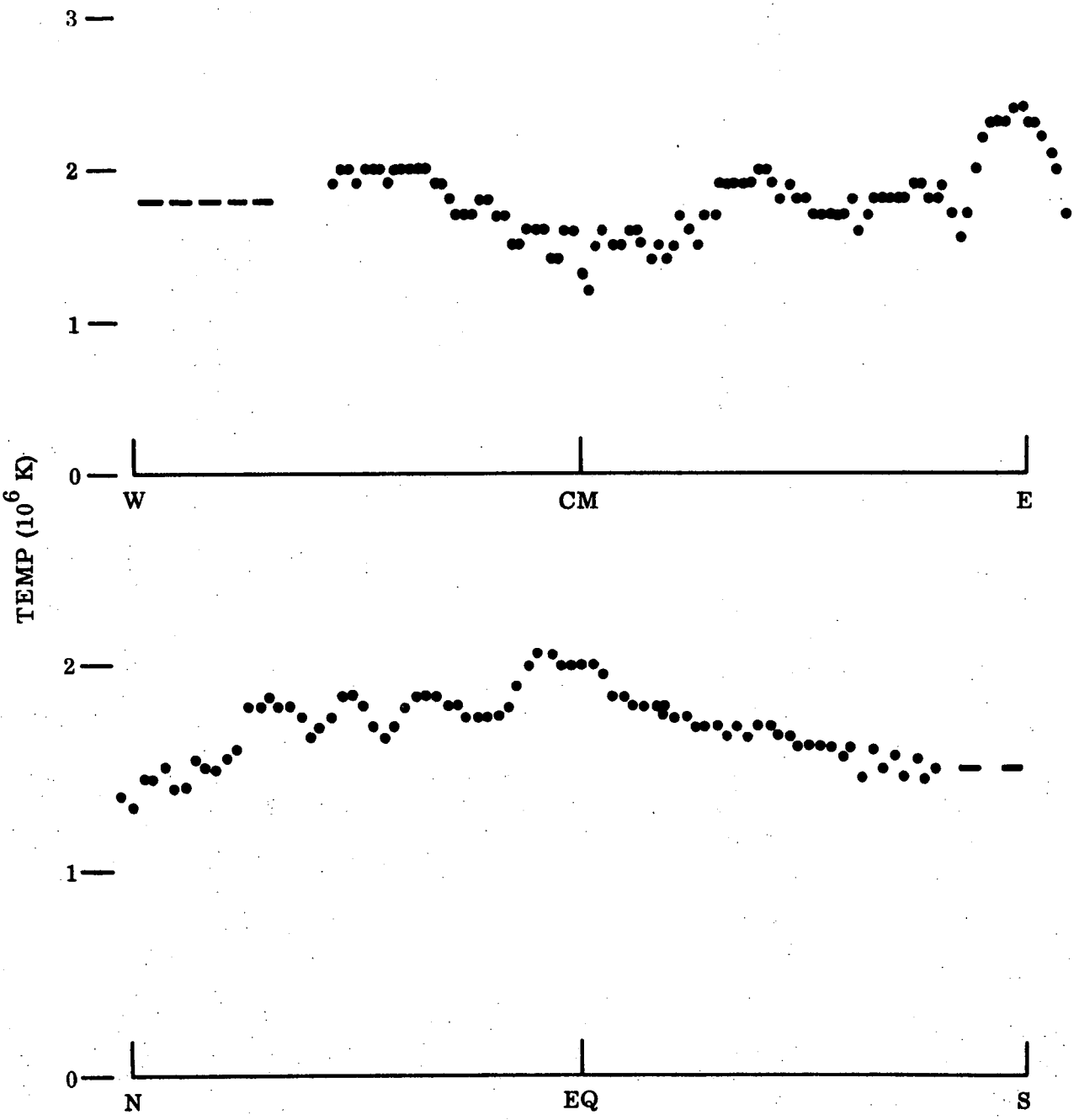

Figure 10 Distribution of coronal temperature based on a W-E scan (top-29 April 1971) and a N-S scan (bottom - 24 April 1972). The active region signals have not been corrected for the general corona contribution.

executing a complex observing program has been established. The inclusion of a time lapse H-alpha aspect camera in the experiment payload has proven to be of very great benefit in determining payload pointing performance and in reducing the experimental data.

Based on experience gained under this contract, we strongly urge that the SPARCS pointing control continue to be improved and applied to solar research. It has demonstrated a basic capability for highly accurate, stable and versatile performance. We also urge that a compact time-lapse aspect camera operating with an H-alpha filter having a bandpass of about 0.75 A be developed for flight as a standard SPARCS accessory. The diagnostic aspect data provided by such a device is invaluable in the event of a flight anomaly or when direct absolute pointing information is required by the experimenter.

It is very important that a high quality, large scale, image of the sun in H-alpha be made available to the experimenter at the rocket launch area in real time. This image is required for assessment of solar activity conditions and for final selection of SPARCS control parameters. Also, if effective coordinated experimental programs involving rocket launches are to be carried out in the future, it is imperative that the telephone service available to experimenters at the WSMR launch areas be improved.

We regret to note that in our solar rocket programs over the past six years there has been an increasing number of formal requirements, reviews and paperwork. These requirements tend to increase the cost of the programs and eat into the productive time of key program personnel. We feel that one of the most beneficial aspects of a rocket program is its relative informality and flexibility, permitting the maximum in innovation and improvement of technique. Thus, we urge that those responsible for mangement of the NASA rocket programs attempt to maximize the informality of necessary controls and to continually scrutinize existing review, control and reporting procedures with a view toward minimizing the unproductive load on the time of key personnel in all organizations.

Finally, we wish to emphasize our satisfaction with the support services we have received throughout this program from NASA and its contractors as well as the launch and recovery support at WSMR. We recommend that all necessary support be made available to permit these groups to continue their important functions to the present high standard.

7. REFERENCES

Catura, R.C., Acton, L.W. and Fisher, P.C., "Localization of Solar X-Ray Emission at Energies above 3 keV," Nature, 227, 55 (1970).

Gabriel, A.H. and Jordan, C., "Interpretation of Solar Helium-Like Ion Line Intensities," Mon. Not. Roy. Astron. Soc., 145, 241 (1969).

Schweizer, W. and Schmidtke, G., "High-Resolution Extreme-Ultraviolet Solar Spectrum Recorded with a Diffraction-Filter Spectrograph," Astrophys. J. Letters, 169, L27 (1971).

APPENDIX 1

A ROCKET-BORNE X-RAY SPECTROMETER/ MONOCHROMATOR SYSTEM FOR MAPPING THE SOLAR CORONA

L. W. ACTON, R. C. CATURA, J. L. CULHANE, and A. J. MEYEROTT
Lockheed Palo Alto Research Laboratory, Palo Alto, Calif., U.S.A.

A rocket payload is being prepared for the purpose of examining the spatial distribution of line emission from two important ions, O VII and Ne IX, in the solar corona. The payload will contain the following integrated set of instruments.

(1) A pair of X-ray spectrometers utilizing KAP crystals of approximately 100 cm^2 area.

(2) An optical aspect camera with a 1 Å bandpass H-α filter to measure the location of the field of view of the X-ray systems on the sun through out the rocket flight.

(3) A collimated proportional counter spectrometer operating in the 3 to 15 keV range.

The two X-ray analysing crystals will view the Sun through collimators which limit their field of view to 1.7 arc min FWHM. Each crystal will be sequentially positioned so as to scan over a narrow wavelength range once each second in 64 steps. The two spectrometers will cover the wavelength intervals containing the helium-like emission lines of O VII (21.6 Å) and Ne IX (13.5 Å) respectively. The diffracted X-rays will be detected by thin-window proportional counters and the accumulated counts will be processed and sent to telemetry by a digital data processor in synchronism with the stepwise crystal scan.

During the rocket flight the SPARCS attitude control system will cause the field of view of the X-ray systems to traverse a 40 arc min path centered on the Sun at an angular rate of approximately 0.33 arc min per second, roll the payload approximately 90° about its longitudinal axis, and then execute a second 40 arc min traverse of the Sun. The spatial traverse rate will allow about 5 s of observing time (corresponding to 5 wavelenth scans by the analysing crystals) per 1.7 arc min on the Sun. The resulting spatially and spectrally resolved data will be used to construct spectroheliograms in each of the 6 spectral lines covered by the spectrometers. The line intensity ratios will be used to compute coronal densities and temperatures.

This program is being carried out under the support of the National Aeronautics and Space Administration (contract NASw-1834) and the Lockheed Independent Research program.

Labuhn and Lüst (eds.), New Techniques in Space Astronomy, 181.

(Reprinted from Nature Physical Science, Vol. 233, No. 39, pp. 75–77, September 27, 1971)

APPENDIX 2

Helium-like Line Emission from Coronal Features

SINCE Gabriel and Jordan[1] proposed the theory relating the relative intensity of the inter-system ($^3P - {}^1S_0$) and forbidden ($^3S_1 - {}^1S_0$) lines of helium-like ions to the electron density of the emitting volume there has been growing interest in using this type of information to determine electron densities in the solar corona[2–5]. We present here the preliminary results of a rocket experiment designed to study the OVII and NeIX line emission from discrete coronal features. These results indicate that electron densities in normal, non-flare, coronal features are below the low density limits (6×10^9 and 1×10^{11} cm^{-3} respectively) given by Freeman *et al.*[5] for these particular ions.

Gabriel and Jordan[1] have shown that the ratio of the forbidden line intensity ($1s^2\ {}^1S_0 - 1s2s\ {}^3S_1$) to the inter-system line intensity ($1s^2\ {}^1S_0 - 1s2p\ {}^3P$) in a helium-like ion may be used to obtain an estimate of electron density for the region in which the emitting ions are located. If steady-state conditions are assumed, this ratio (R) is related to the electron density (N_e) by the expression

Table 1 Values of R and N_e*

Ion	Temperature of maximum resonance line emission	Values of R and N_e* calculated by Freeman *et al.*[5]		Value of R observed in the present experiment (whole disk)
	(K)	(N_e*)	(R)	
OVII	1.9×10^6	6.0×10^9	3.6	3.58 ± 0.04
NeIX	3.5×10^6	1.3×10^{11}	3.0	3.02 ± 0.07

More recently, Freeman *et al.*[5] have recalculated N_e* using modified values for the $2\ {}^3S$ to $1\ {}^1S$ transition probability. They derive these values using a Z scaling law with a Z^{10} dependence rather than the Z^8 dependence suggested by Greim[9] and obtain the proportionality constant from the observed R value for CV. Their revised values of N_e* are given in Table 1 for the OVII and NeIX ions. The new values

$$R = \frac{A\,(2\ {}^3S \rightarrow 1\ {}^1S)}{[N_e\,C\,(2\ {}^3S \rightarrow 2\ {}^3P) + \Phi][1 + F] + A(2\ {}^3S \rightarrow 1\ {}^1S)\begin{bmatrix} 1 + F & \\ B & -1 \end{bmatrix}} \qquad (1)$$

where the C terms are electron collisional excitational rates, the A terms are transition probabilities and Φ is the photo-excitation rate for the $2\ {}^3S$ to $2\ {}^3P$ transition. The parameter F is the ratio of the electron collisional excitation rates and

$$F = \frac{C\,(1\ {}^1S \rightarrow 2\ {}^3S)}{C\,(1\ {}^1S \rightarrow 2\ {}^3P)} \qquad (2)$$

B is the branching ratio from the ^3P states to the ground state.

Using these equations, Gabriel and Jordan[1] have calculated the relationship between R and N_e for several helium-like ions including OVII and NeIX. For small values of N_e, R assumes a limiting value but, at higher electron densities, exhibits a measurable variation the magnitude of which depends on the Z value of the ion in question. Gabriel and Jordan[1] have characterized this higher electron density as the density (N_e*) for which R is reduced by 10% of its value at the low density limit. For helium-like ions with $Z \geq 8$ (that is OVII) the photo-excitation rate Φ will be small. Using this assumption, Gabriel and Jordan[1] have calculated N_e* for several helium-like ions. The A values used were obtained from the work of Wiese *et al.*[6], Drake and Dalgarno[7], Garstang[8] and Greim[9]. They computed the value of $C(2\ {}^3S \rightarrow 2\ {}^3P)$ from the formula given by Van Regemorter[10] with the assumption that each ion existed at the temperature for which its resonance line emission was a maximum[11]. The value of F, obtained from a number of measurements of R on the Sun, was taken as 0.35. This seems to be acceptable for non-flare conditions.

are 30 and 400 times greater than those previously calculated. Although the photo-excitation rate for the $2\ {}^3S$ to $2\ {}^3P$ transition is small for these ions, Blaha[12] has suggested that collisional excitation of this transition by protons and α-particles may become important at high temperatures. At the temperatures of maximum resonance line emission from OVII and NeIX, he finds the proton collisional excitation rates to be 7% and 16% of the respective electron collisional excitation rates. Although these calculations show that the proton excitation rate makes a small contribution, the conditions in solar active regions may be such that both ions exist above their temperature of maximum abundance. This situation may lead to a significant temperature dependence of the parameter F in equation (1). Both these points should be considered in future applications of the theory to data of high statistical and experimental precision.

Our instrument and planned observing programme have been described in outline[13] and will be discussed in more detail elsewhere. The instrument utilized two collimated Bragg crystal spectrometers covering the helium-like "triplets" of OVII and NeIX at 22 Å and 13.5 Å respectively. The fields of view of the plane KAP analysing crystals were defined by Oda type collimators with a full width of 1.7 arcmin at half maximum transmission. A SPARCS attitude control system caused the fields of view to traverse the solar disk at an average rate of approximately 0.3 arcmin s^{-1}. During this traverse each analysing crystal was rocked through its spectral range once a second. Instrument aspect and field of view were

recorded four times each second by an on-board H-alpha telescope and camera.

Fig. 1 illustrates the circumstances of the observations, the nature of the data and our preliminary results on the forbidden to inter-system line ratios. Fig. 1*c* is an H-alpha photograph of the Sun obtained 10 min after the flight. The path of the scan and FWHM field of view of the crystal spectrometers are indicated. The rocket did not fully stabilize until after the scan was initiated so that the data from the first 7 arcmin of the traverse are unavailable until aspect corrections are made. The traverse of the disk was not uniform but was in the form of an oscillatory 30 arc s advance followed by a 20 arc s retreat with a period of approximately 1.1 s. Preliminary corrections for this motion indicate that it should not cause significant error in *R*.

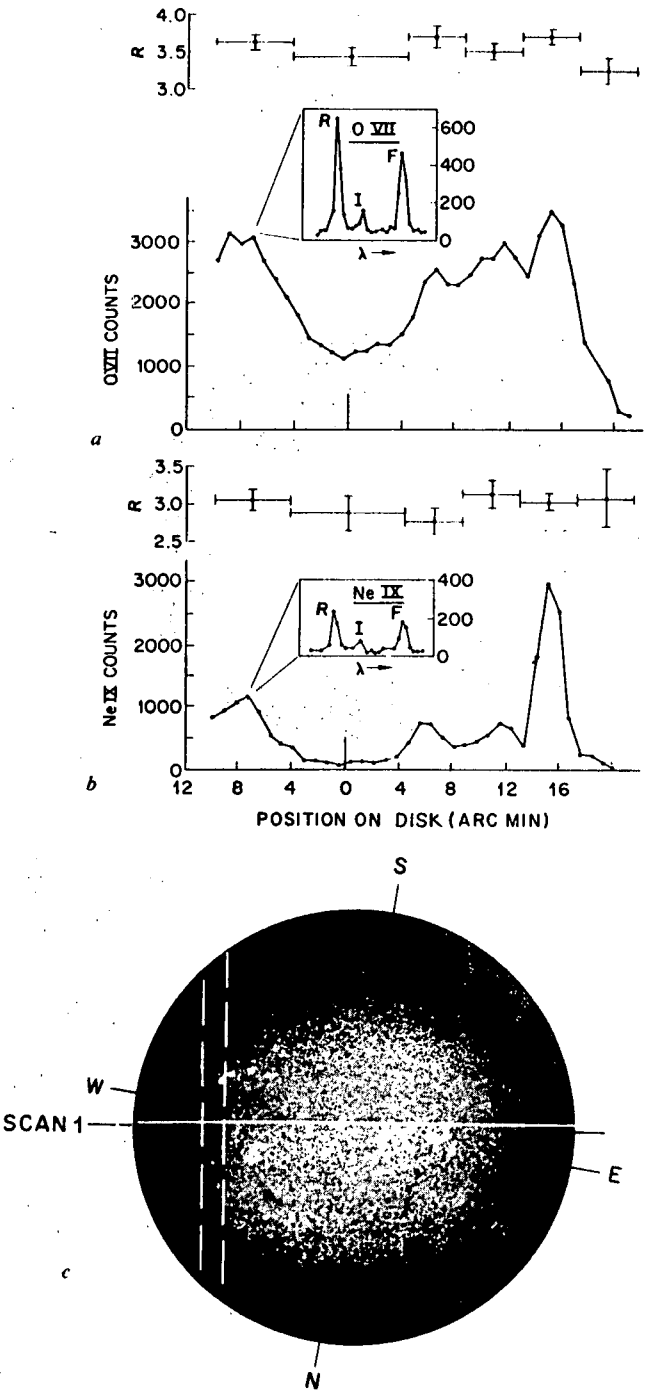

Fig. 1 *a*, The ratio *R* and the counting rate for the resonance, inter-system and forbidden lines of OVII plotted against position on the solar disk. Inset, An OVII spectrum obtained by the crystal at the disk position indicated. *b*, Similar data obtained from the NeIX system; *c*, solar disk photograph in Hα with the scan direction and the crystal spectrometer field of view indicated.

Figs. 1*a* and *b* show equivalent data from the OVII and NeIX systems respectively. The lower curve in each part shows the variation in the X-ray line emission (resonance, inter-system and forbidden lines summed and background subtracted) across the disk. The correlation with H-alpha plage regions is obvious. The small, strongly emitting, region near the east limb had been the site of some flare and surge activity during the preceding half hour. Both the ratio of neon-to-oxygen emission and the data from a collimated proportional counter spectrometer indicate the presence of higher temperature material in this feature.

The insets in Figs. 1*a* and *b* illustrate the quality of the X-ray spectral data used in this analysis. The spectra shown were acquired during a 2 s interval at the indicated position on the traverse of the disk. The horizontal bars on the *R* plots indicate the spatial extent of the data included in each value and the vertical error bars indicate one standard deviation.

The use of a collimated crystal spectrometer allows the separation of active and quiet emission. The measured values of *R* were constant at the low density limit within experimental error, for the quiet corona and the five individual active regions observed. Averaged values of *R*, computed from data from the whole disk, are compared with the theoretical values of Freeman *et al.*[5] in Table 1. Although the oscillations in the disk traverse discussed above can affect the measurement of line ratios (by altering the angle between an active region and the crystal collimator) we do not believe that this effect has masked any variation in *R*.

In the absence of variation in the ratio *R*, as determined from the OVII lines, we conclude that the electron density in all coronal regions observed was less than 6×10^{9} cm^{-3}. The absence of variation in the NeIX ratio is of course consistent with this result. Rugge and Walker (ref. 14 and work to be published) have obtained values of *R* from OVII line observations of the whole Sun with satellite-borne crystal spectrometers. The values that they determined show no variation during an extended period of time in 1966–67 and a brief period in 1969. Our work complements these observations and also shows that the electron densities in the parts of corona that emit OVII radiation are consistently less than 6×10^{9} cm^{-3}. Because the whole disk was scanned with a collimated instrument, the conclusion applies to both active and quiet coronal regions. Preliminary temperature estimates, obtained from the OVII to NeIX resonance line ratios, indicate that the temperature varies between approximately 1.8×10^{6} K and 2.9×10^{6} K for the quiet corona and for the most intense X-ray features observed, respectively.

We wish to acknowledge the important contribution to this experiment made by E. C. Gabris of NASA-Ames, who was responsible for the SPARCS pointing control and vehicle instrumentation, and of G. Carroll and H. Ramsey of Lockheed Solar Observatory, who prepared the H-alpha flight telescope. We wish to thank Dr R. J. Liefeld for many helpful discussions. This research has been supported by NASA and by the Lockheed Independent Research Programme.

L. W. Acton
R. C. Catura
A. J. Meyerott

Lockheed Palo Alto Research Laboratory,
Palo Alto,
California

J. L. Culhane

Mullard Space Science Laboratory,
Physics Department,
University College London

Received September 10, 1971.

[1] Gabriel, A. H., and Jordan, C., *Mon. Not. Roy. Astron. Soc.*, **145**, 241 (1969).
[2] Walker, A. B. C., and Rugge, H. R., *Astron. Astrophys.*, **5**, 4 (1970).
[3] Batstone, R. M., Evans, K., Parkinson, J. H., and Pounds, K. A., *Solar Phys.*, **13**, 389 (1970).
[4] Doschek, G. A., Meekins, J. F., Kreplin, R. W., Chubb, T. A., and Friedman, H., *Astrophys. J.*, **164**, 165 (1971).
[5] Freeman, F. F., Gabriel, A. H., Jones, B. B., and Jordan, C., *Proc. Roy. Soc.*, A (in the press, 1971).
[6] Weise, W. L., Smith, M. W., and Glennon, B. M., *Atomic Transition Probabilities*, NSRDS-MBS 41 (US Government Printing Office, 1966).
[7] Drake, G. W. F., and Dalgarno, A., *Astrophys. J.*, **157**, 459 (1969).
[8] Garstang, R. H., *Astrophys. J.*, **148**, 579 (1967).
[9] Greim, H. R., *Astrophys. J.*, **156**, L103 (1969).
[10] Van Regemorter, H., *Astrophys. J.*, **136**, 906 (1962).
[11] Jordan, Carole, *Mon. Not. Roy. Astron. Soc.*, **142**, 501 (1969).
[12] Blaha, M., *Bull. Amer. Astron. Soc.*, **3**, 246 (1971).
[13] Acton, L. W., Catura, R. C., Culhane, J. L., and Meyerott, A. J., *New Techniques in Space Astronomy* (edit. by Labuhn and Lust), 145 (Reidel, Dordrecht, 1971).
[14] Rugge, H. R., and Walker, jun., A. B. C., *Solar Phys.*, **15**, 372 (1971).

Printed in Great Britain by Flarepath Printers Limited, Watling Street, Colney Street, St. Albans, Herts.

APPENDIX 3

MAPPING THE SOLAR CORONA IN X-RAY LINES OF OVII AND NEIX

R. C. CATURA, L. W. ACTON, and A. J. MEYEROTT
Lockheed Palo Alto Research Laboratory Palo Alto, Calif. 94304, U.S.A.
and
J. L. CULHANE
Mullard Space Science Laboratory, University College London

Some preliminary results of a rocket experiment, which utilized collimated Bragg Crystal spectrometers to map solar X-ray line emissions from He-like ions of oxygen and neon are presented. The two spectrometers used KAP crystals with a common field of view 1.7′ FWHM in the narrow dimension. The spectrometers were scanned

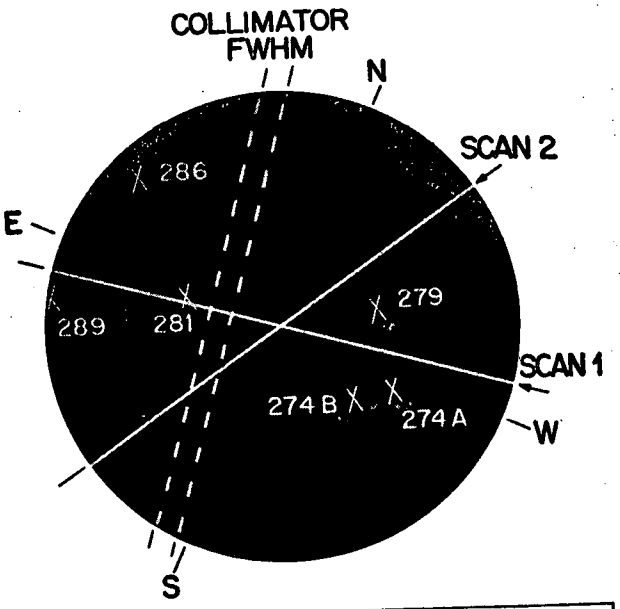

Mc MATH PLAGE	TEMP (°K)	EMISSION MEASURE (CM^3) $\int N_e^2\, dV$	R VALUES	
			O VII	Ne IX
274 A	2.4×10^6	1.5×10^{47}	3.4	2.9
279, 274 B	2.7×10^6	1.6×10^{47}	3.7	3.2
281	2.5×10^6	1.3×10^{47}	3.6	2.8
286	2.4×10^6	1.4×10^{47}	3.5	3.3
289	2.9×10^6	3.8×10^{47}	3.7	3.1
GEN. CORONA	1.8×10^6	1.3×10^{45} /(ARC MIN)^2	3.4	2.9

Fig. 1. Location of the emitting regions as determined from two fan beam scans of the disk are shown by crosses on a Hα photograph of the Sun. The scan paths, the relative size of the collimator field of view, and parameters evaluated by this experiment are also shown.

in wavelength once each second to observe the resonance, intersystem and forbidden lines of O VII and Ne IX.

The spatial distribution of these line emissions was measured on April 29, 1971 near 1630 UT and has been resolved into contributions from at least six regions of activity on the sun. By utilizing intensities of the O VII and Ne IX resonance lines and assuming an isothermal plasma we have calculated the temperature of each region and the corresponding value of emission measure ($\int N_e^2 \, dv$). The parameter R, the ratio of forbidden ($^3S_1$–$^1S_0$) to intersystem (^3P–$^1S_0$) line intensities, has also been calculated.

These data are shown in Figure 1. Values for the general corona were obtained when the field of view was free of plage areas and represent averaging over a 1.7′ wide strip extending approximately from pole to pole. Values of KAP crystal reflectively have been obtained from the measurements of Liefeld *et al.* (1970). The abundances of oxygen and neon used for these calculations were provided by Drs Dupree and Withbroe and are coronal values derived from XUV data obtained by the Harvard experiment on OSO 4

No significant variation of the value R is found from feature to feature on the disk. According to a recent paper by Freeman *et al.* (1971), this places an upper limit of 6×10^9 cm^{-3} on the electron density in the coronal regions observed in the experiment.

Acknowledgements

This work was supported by the National Aeronautics and Space Administration under Contract NASw-1834 and by the Lockheed Independent Research Program.

References

Freeman, F. F., Gabriel, A. H., Jones, B. B., and Jordan, C. 1971, *Phil. Trans. Roy. Soc. London* **A270**, 127.

Liefeld *et al.*: 1970, *Adv. X-Ray Analysis* **13**, 378.

DISCUSSION

A. B. C. Walker: Can you obtain an integrated emission measure for the entire disk by summing your data?

R. C. Catura: We have not yet analysed some low intensity emission from several plages near the west limb. When this analysis is completed we can obtain the emission measure for the entire disk.

S. R. Pottasch: To get good agreement for $N_e^2 V$ from the oxygen and neon lines you only need the correct O:Ne ratio and not the absolute values with respect to hydrogen. What value of the O:Ne ratio did you use?

R. C. Catura: In this analysis we have used coronal values of O and Ne abundance which were obtained by Dr Dupree of Harvard College Observatory. These values give an O:Ne ratio of 20.

APPENDIX 4

CORONAL SURVEY IN X-RAYS OF O VII AND Ne IX

L. W. Acton, R. C. Catura, A. J. Meyerott* and C.J. Wolfson

Lockheed Palo Alto Research Laboratory
Palo Alto, California

J. L. Culhane

Mullard Space Science Laboratory
Physics Department
University College London

* We are saddened to report the death of A.J. Meyerott on 13 November 1971.

CORONAL SURVEY IN X-RAYS OF O VII AND NE IX

Acton, et al.

Insert (Page 7)

The crystal rotation rate W is 0.053 and 0.018 rad s^{-1} for the O VII and Ne IX systems, respectively and the numerical value of the parameter t is 0.3. The parameter A and p have the values 52 and 0.095 for the O VII and 51 and 0.42 for the Ne IX system.

Note Added In Proof

It has been pointed out to us by Dr. Carole Jordan that the mean emission temperature $< T_{\lambda} >$ for O VII given in Table III for the general corona (i.e., 1.25×10^6 K) may be unrealistically low because its determination is unduly influenced by the low temperature end of the exponential emission measure distribution (Equation 4). Physically, this is a valid criticism. However, it is not possible to devise any distribution of emission measure, including an exponential distribution arbitrarily truncated on the low temperature end, which may be used with our data to obtain a mean emission for O VII higher than that derived from an isothermal model (i.e., 1.45×10^6 K).

ABSTRACT

We report some results of a rocket experiment flown on 29 April 1971. A survey of the solar corona was carried out with a pair of collimated Bragg spectrometers to study the resonance, intersystem and forbidden line emission from the helium-like ions O VII (22 A) and Ne IX (13 A). In the direction of dispersion, the collimator provided a fiew of view of 1.7 arcmin. Also, the continuum radiation near 3 A was monitored by a collimated proportional counter within a view angle of 4.2 arcmin. The observed X-ray emission came from the general corona, seven plage regions, and one dynamic feature -- the late stage of a small flare. From the intensity of the O VII and the Ne IX resonance lines the electron temperature and emission measure of the individual emitting regions are derived on the basis of two models, one (a) in which the region is assumed to be isothermal and another (b) in which the emission measure decreases exponentially with increasing temperature. The latter model, which is the most adequate of the two, yields for the electron temperature of the time-varying feature 2 to 3 x 10^6 K, for the other active regions 1.5 to 2.5 x 10^6 K, and for the general corona 1.3 to 1.7 x 10^6 K. The Ne IX emitting regions are about 1.5 times as hot as the O VII regions. The emission measure ranges from 0.4 to 2.3 x 10^{48} cm^{-3} for all active regions and is about 2 x 10^{49} cm^{-3} for one hemisphere of the general corona above 10^6 K. From an analysis of the ratio, R, of the forbidden and intersystem lines of O VII, we conclude that none of the regions producing these lines at the time of the rocket flight had electron densities exceeding about 3 x 10^9 cm^{-3}. Our data demonstrate a dependence of R upon temperature in agreement with the theory of Blumenthal et al. (1971). The wavelengths for the intersystem, the $1s^2 2s\ ^2S^e$ - $1s2p2s\ ^2P^o$ satellite, and the forbidden transitions show in the case of Ne IX improved agreement with predictions. The observed strength of the satellite line for both O VII and Ne IX agrees with the predictions of Gabriel's (1972) theory, which attributes their formation to dielectronic recombination.

1. Introduction

The observation of emission lines of highly ionized atoms provides a powerful means for studying the plasma of the solar corona. Many experiments for this purpose have been carried out with uncollimated plane Bragg spectrometers. Recent work includes that of Evans and Pounds (1968), Batstone et al. (1970) and Rugge and Walker (1970, 1971). All of these experiments respond to the sun by convoluting the spatial and spectral distribution of the radiation. Parkinson (1971) has reported results of the first solar experiment with a collimated Bragg spectrometer.

In this paper we report some results of a coronal survey carried out with an X-ray spectrometer system which permitted the study of individual active regions and the general corona. In this experiment a pair of large area, collimated crystal spectrometers were used to study the resonance, intersystem and forbidden line emission from the helium-like ions O VII and Ne IX. An Oda-type collimator provided a one-dimensional "fan beam" field of view of 1.7 arcmin full width at half maximum (FWHM) in the plane of dispersion by several degrees FWHM in a direction perpendicular to the dispersion plane. While the two crystals scanned over the three lines from each of these ions, the field of view passed slowly across the solar disc twice at different heliocentric angles. The experiment was flown on a NASA-Aerobee 170 rocket from White Sands Missile Range and collected data from approximately 16.32 U.T. to 16.37 U.T. on 29 April 1971.

2. Instrumentation

The instrumentation is unique in increasing sensitivity, spatial and spectral resolution at the expense of spectral range (Acton et al., 1971a). Figure 1 shows a schematic representation of the payload. The two plane KAP crystals (97 cm^2 each) were mounted below the large X-ray collimators and were rotated independently in 64 steps through the small range of Bragg angles necessary to cover the wavelength ranges 21.38 to 22.27 A(O VII) and 13.34 to 13.78 A (Ne IX). The crystal rocking period was one second for the 64 steps. Photons diffracted from the two crystals were registered in proportional counters (crystal detectors) which remain fixed because of the small crystal motion. Pulses from these proportional counters were passed through window discriminators

to reduce the background rate before being accumulated and telemetered 64 times per second in synchronism with the stepper motors which rotate the crystals. The crystal detectors were continuously calibrated in flight with weak Fe^{55} sources. These calibration X-rays did not contribute to the spectrometer counting rates because of amplitude discrimination. In addition, the resonance line photon energies of 0.575 keV for O VII and 0.923 keV for Ne IX provided excellent calibration during flight.

The rocket pointing control (SPARCS system) advanced the field of view across the solar disc at a nominal rate of 0.3 arcmin per sec. During each complete spectral scan by the two crystals, the rocket axis moved 0.3 arcmin or 18 percent of the collimator field of view of 1.7 arcmin FWHM. Light entering an aspect aperture was directed through an H alpha filter-telescope combination with a nominal 1 A bandpass and produced a solar image on SO-392 film. An area of additional exposure approximately 4 arcmin wide was superimposed on the solar image by light passing through the X-ray collimator grids. The location of this feature on the solar image was identical to that of the X-ray field of view on the sun. The camera was operated at a rate of four frames per second so the motion of the collimator field of view across the solar disc could be followed throughout the flight.

A beryllium window proportional counter sensitive in the wavelength range 0.8 to 4.0 A was included in the payload. The field of view of this detector in the direction of the spatial scan was 4.2 arcmin FWHM and was parallel to the 1.7 arcmin field of view of the crystal spectrometers. Pulses from this proportional counter were analyzed in six differential pulse height channels. Counts were accumulated in these channels and telemetered in digital form once each second.

The payload also carried an ultraviolet spectrograph utilizing a diffraction filter entrance slit. This spectrograph was provided by the Arbeitsgruppe fur Physikalische Weltraumforschung, Freiburg, Germany. Preliminary results of their high resolution spectra in the 180 A region have been reported by Schweizer and Schmidtke (1971).

3. Coronal Source Distribution

An H-alpha photograph of the disc, taken near the time of flight by the Lockheed Solar Observatory, is shown in Figure 2. The common field of view of the crystal spectrometers (FWHM) is represented by a pair of dashed lines. It was moved across the disc on two separate scans by the SPARCS attitude control system. The scan directions are indiciated by the solid lines superimposed on the photograph. A number of plage regions are visible in Figure 2. The only transient activity on the disc at the time of flight came from a small flare (-F) which occured about 30 minutes before launch in McMath Plage No. 289 near the east limb. This small dynamic feature will be discussed in detail in a later publication. No impulsive X-ray or radio events have been reported during the flight.

The wavelength resolution of the spectrometers is indicated in Figure 3 which shows spectra of both O VII and Ne IX. The spectra in this Figure were obtained during a 5 second time interval from the X-ray active region associated with plage No. 281. The resonance ($1s^2\ ^1S$ - $1s2p\ ^1P_1$), inter-system ($1s^2\ ^1S_o$ - $1s2p\ ^3P$) and forbidden ($1s^2\ ^1S_o$ - $1s2s\ ^3S_1$) transitions are labelled. In 5 seconds, the rocket axis moves 1.5 arcmin across the disc, a distance approximately equal to the full width at half maximum of the collimator field of view. The data of Figure 3, therefore, demonstrate the typical sensitivity and wavelength resolution of the experiment with counts registered from one instrument field of view.

Plots of counting rate against position on the disc are shown in Figures 4 and 5 for both crystals and the proportional counter. In Figure 4, the emission from the three lines (R, I and F) has been added together for the O VII (Figure 4a) and Ne IX (Figure 4b) ions and plotted against disc position for the first rocket scan. The counting rate from four of the proportional counter energy channels (3.2 to 7 keV) is similarly plotted in Figure 4c. Data obtained during the second scan are plotted in Figure 5a and b. The O VII detector suffered an unexplained increase in counting rate shortly after the start of the second scan and so data from these lines on the second scan are not available.

When the spectrometer's field of view was near the center of the disc during the first scan, the collimators were pointed at a region free from plage activity. For both the O VII and Ne IX data, the counting rates dropped to a minimum at this time as shown in Figure 4a and b. The points marked by squares (□) in Figure 4a show how this signal from the "general corona" would be modified as the fan beam field of view is moved away from the center of the disc to include less of the corona assuming the general coronal emission is uniform for the entire disc.

It may be seen from Figure 4 that X-ray active regions are more easily resolved in Ne IX radiation than in the radiation of O VII. This is because the general coronal temperature is close to the temperature of maximum abundance for O VII. In active regions, the relative emissivity of Ne IX is increased. For this reason, and because data were available from two scans, the location of the active regions was carried out using the Ne IX counting rates. The signal from the general corona was determined as described above and subtracted from the total counting rate at each point on the disc to determine the contribution of the active regions. The emission observed near the beginning of both scans comes from near the northwest limb and was presumed to be from several diffuse plages in that area. These data were treated as a unit for calculative purposes and no further attempt was made to spatially resolve them. The other active region data were fitted to the triangular response of the collimator with the assumption that the regions were small compared to the 1.7 arcmin collimator field of view. This process was carried out with Ne IX data from both scans and source locations on each scan were transferred to an H-alpha photograph as a series of straight lines. The points of intersection of these lines were correlated with H-alpha features. The McMath numbers of the correlated plages are shown in Figures 4b and 5a. The source locations were then transferred to the O VII plot and the amplitude of the contribution from each active region was determined. For at least two of the regions, (286 and 289) the triangular response of the collimator does not provide a good fit to the data. Perhaps the assumption that the source size is small compared to the collimator field of view is no longer valid for O VII because the emitting regions may be more diffuse at the

lower temperatures where this ion is most abundant. This point will be discussed further in connection with the values calculated for emission measure.

The source locations, obtained from the Ne IX data as described above, are shown in Figure 6. A McMath-Hulbert calcium report for the previous day (April 28) is shown since no data have been published for the day of the flight. Regions 265, 266 and 271 have moved onto the west limb by April 29 and are probably responsible for the diffuse emission observed near the beginning of both scans.

Measured values of R, the ratio of the forbidden (F) to intersystem (I) line intensities are plotted in Figure 4 at various positions across the disc for both the Ne and O data. No variation is found in this ratio which may be attributed to especially high density regions (Acton et al., 1971b).

Figures 4c and 5b show data from the collimated proportional counter. These data show the dominance of the small dynamic feature at higher photon energies. The emission from region 289 at these energies is at least ten times that of any other region on the disc. The emission in the 3.2 - 7 keV band from this feature decreases by about 20 percent in the two minutes separating scans one and two.

4. Plasma Parameters

The intensity of the O VII and Ne IX resonance lines may be used to obtain information on the electron temperature and emission measure of the emitting regions. The number of counts recorded in a line during one rotation of the crystal is given by:

$$N_\lambda = F_\lambda \frac{R_\lambda}{W} \; t \; A_\lambda \; p_\lambda, \qquad (1)$$

where N_λ is the integrated number of counts in the line per crystal scan, F_λ is the photon flux at wavelength λ in photons $cm^{-2} sec^{-1}$, R_λ is the integrated reflection coefficient of the crystal in radians, W is the angular

rotation rate of the crystal in radians sec^{-1}, t is the transmission of the collimator, A_λ is the effective area of the crystal in cm^2 when it is set at the correct Bragg angle for the diffraction of X-rays of wavelength λ, and p_λ is the photon detection efficiency of the proportional counter used to register the photons diffracted from the crystal. The subscript, λ, is used to denote parameters which are wavelength dependent. The intrinsic line width is assumed small compared with the crystal rocking curve in all cases -- a valid assumption for Doppler broadened lines from the coronal plasma incident on KAP crystals.

For the present analysis, we have used the KAP crystal reflection coefficients measured by Charles (1968) and by Blake (1971 private communication). These are 1.8×10^{-5} and 5.5×10^{-5} radians for the O VII and Ne IX spectrometers, respectively.

Table I presents the observational data obtained by this experiment. The counts given represent the total observed in one crystal rotation when the source is centered in the collimator field of view. The general coronal signal has been subtracted as described above and the stated errors primarily represent the uncertainty in this process. In the case of the general corona, the errors reflect only counting statistics.

In order to determine temperature dependence of the ratio of O VII to Ne IX resonance line fluxes, it is necessary to calculate the emissivity of a coronal plasma. On the assumption that every collisional excitation of a resonance transition is followed with spontaneous decay by photon emission the line flux may be calculated with the aid of an approximate expression for the electron collisional excitation rate. The $\bar{g}$ approximation (Van Regemorter, 1962; Seaton, 1964) for the line flux is given by:

$$F_\lambda = 5 \times 10^{-31} \bar{g} f_\lambda \varphi_\lambda^{-1} A_z \int M A_i T^{-0.5} 10^{-(5040 \varphi_\lambda / T)} dT \quad (2)$$

photons $cm^{-2} sec^{-1}$ at earth.

In this expression, $\bar{g}$ is the temperature averaged Gaunt factor (which has been set equal to 0.3), f_λ is the oscillator strength of the line,

φ_λ is the photon energy in electron volts, A_z is the elemental abundance relative to hydrogen, M is the differential emission measure, T is the electron temperature in degrees Kelvin ; to be consistent with our definition of M, the integration step dT has the dimension 10^6 K. A_i is the ion abundance at temperature T. Values of A_z for neon (2.8×10^{-5}) and oxygen (5.9×10^{-4}) were obtained from Dupree (1971 private communication). The ionization balance calculations of Joran (1969) provided the temperature dependent ion abundances. The numerical constant includes a factor relating the electron and hydrogen densities. The constant given is for a helium abundance of about 0.1.

The emission measure of a volume is normally defined as $\int N_e^2 dV$, the integral of the square of the local electron density over the volume of interest. The local electron density, N_e, may alternatively be expressed as a function of the local electron temperature within the volume of interest. Thus, the differential emission measure, M(T), is defined:

$$M(T) = \frac{d}{dT} \int N_e^2 \, dV \quad cm^{-3} \, (10^6 \, K)^{-1}. \qquad (3)$$

With two resonance line intensities and equations (1) and (2), one may derive two parameters descriptive of the coronal plasma. For instance, if an isothermal model is assumed, the ratio of line intensities may be used to derive the electron temperature. The temperature is put back into the equations along with the absolute flux of either line to give the corresponding emission measure. Alternatively, one may assume some functional form for the differential emission measure and use the observations to solve for the functional parameters.

We have analyzed the data by both methods. For the emission measure distribution in the non-isothermal case, the exponential expression:

$$M(T) = C \cdot 10^{-T/To} \, cm^{-3} \, (10^6 \, K)^{-1} \qquad (4)$$

proposed by Chambe (1971) has been adapted. Here T is the electron temperature and the constants C and T_o, which are related to the total

emission measure and the steepness of the emission measure distribution, are parameters determined from the analysis. Such a distribution appears to be consistent with the data of Batstone et al. (1970). However, the value for T_o which we derive from their data on three active regions is approximately 7 x 10^6 K, a value somewhat higher than Chambe's 1.5-3 x 10^6 K.

In Figure 7, the calculated O VII/Ne IX resonance line ratio for our spectrometers is plotted versus T (for the isothermal case) and T_o (for the exponential distribution). Note that in the case of the exponential distribution of emission measure, the minimum ratio is more than ten times larger than in the isothermal case. This is a consequence of the large amount of low temperature material always present to produce the O VII line in this model.

The results of the isothermal approximation are given in Table II. The derived electron temperatures have a formal uncertainty of about 10^5 K arising from the experimental errors in the data of Table I. The inadequacy of the isothermal model and possible systematic errors introduce additional uncertainty in the derived plasma parameters. The electron temperatures of the quiescent active regions cluster about a common value with the general corona substantially cooler. The emission measure for the general corona contains a factor of 20 relating our field of view to the whole coronal hemisphere on the basis of a spherically symmetric model. The general coronal temperature is consistent with that derived by Jordan (1966) with EUV data but below the value of 1.8 x 10^6 K obtained by Withbroe (1971) from a study of Li-like line ratios. Widing and Sandlin (1968) have found that the spectrum in the 61-110 A region is best fitted to a general coronal temperature of 1.4 x 10^6 K but comment that all of their data cannot be fitted by an isothermal model. The temperature of 2.4 x 10^6 K and the associated emission measure for the dynamic feature of region 289 are insufficient to produce the observed emission at energies from 3.2 to 7 keV. Material at a considerably higher temperature is required to explain this emission which serves to emphasize the inadequacy of the isothermal model.

The temperatures given in Table II for the isothermal model are in general lower than the preliminary values given by Catura et al. (1972) on the basis of the same experimental data. The reason for the difference is that the earlier values were derived using the peak KAP crystal reflectivities of Liefeld et al. (1970). Liefeld's results are based on measurements using a double crystal spectrometer. A correction for polarization effects and convolution of the two rocking curves must be applied if these data are to be used in analysis of single crystal measurements. When such corrections are applied, there remains a disagreement of a factor of approximately two between the reflection coefficients of Liefeld et al. (1970) and those of Charles (1968) and Blake (1971 private communication). Because of this confusion, and because of the difficulty in relating two crystal measurements to collimated single crystal measurements, we have chosen to reinterpret our data on the basis of integrated reflection coefficients as given by equation (1). This approach also facilitates comparison with earlier work.

The exponential distribution of emission measure in equation (4) (Chambe, 1971) provides a means for treating the emission of non-isothermal regions. The data of Table I and the appropriate curve of Figure 7 have been used to derive the parameters given in Table III for each region. Although T_o has the dimensions of a temperature, it is merely a scaling factor and its absolute value depends on the choice of 10 as the base of the exponential function. Once T_o has been determined, the observed intensity in the resonance line and the solution of equations (1), (2) and (4) may be used to determine the constant C of equation (4).

The mean emission temperature, $< T_\lambda >$, for each ion is defined as:

$$< T_\lambda > = \frac{\int T\, B_\lambda \, dT}{\int B_\lambda \, dT} \; K, \qquad (5)$$

where B_λ is the integrand of equation (2) with M in the form of equation (4). The emission measure for each ion, EM_λ, is given by:

$$EM_{\lambda} = \int_{T_1}^{T_2} M \, dT \quad cm^{-3} \tag{6}$$

where the limits of integration have been arbitrarily set at the temperatures where the emissivity of the gas for the particular resonance line is ten percent of its peak value. The emission measure defined in this way has a wavelength dependence which enters through these limits of integration. The total emission measure of each region, EM_{tot}, is obtained by integrating equation (6) from 10^6 K to ∞. The lower temperature limit is arbitrarily set to approximate the temperature at the base of the corona.

The errors in T_o are in general unsymmetrical because of the shape of the curve in Figure 7. These errors are on the average 30 percent on the high temperature side and 15 percent on the lower temperature side. The mean emission temperatures given in Table III are in general determined to better than ten percent and the emission measures to about plus or minus fifty percent.

Because the exponential function of equation (4), the basis of our non-isothermal model, decreases monotonically toward higher temperatures, the derived emission measures of Table III are naturally greater for O VII, the ion formed at the lower temperature. However, this result is consistent with the data of Figure 4, which show that the O VII regions are larger than the Ne IX regions, relative to our 1.7 arcmin FWHM field of view. For example, taking a typical O VII emission measure of 1.6×10^{48} cm^{-3} and a mean emission temperature of 1.6×10^6 K from Table III and an electron density of 2×10^9 cm^{-3} from the results of Section 5, and assuming a uniform source region one scale height (3.5×10^4 km) thick, we find that the characteristic lateral dimension of the O VII regions are of the order of two minutes of arc. For a similar geometrical model and electron density, the characteristic lateral extent of the Ne IX regions turns out to be about one minute of arc. Such source sizes are consistent with the data of Figure 4. These results are not unique to the particular non-isothermal model chosen, but it is clear

that a model is required for which the source regions are more compact at shorter wavelengths.

5. Spectra

The high sensitivity of our instrument has provided spectra of high statistical accuracy. Also, the narrow collimation employed limited degradation of the spectra resulting from source extent. For this study, the spectra of Figure 8 have been obtained by summing together all useable data from the flight, excluding only that from the dynamic feature associated with plage 289.

Analysis of these spectra is complicated by the possible presence of unknown line blends in the data and by lack of precision in the published wavelengths of the known lines. Furthermore, we do not have a detailed rocking curve for the flight crystals and attempts to derive such a curve from the flight spectra have been only partially successful. The rocking curve is found to be unsymmetrical; near the peaks the line profiles drop off more steeply on the long wavelength side in agreement with theory (Compton and Allison, 1935).

Results of our analysis are presented in Table IV. Except where noted, the wavelengths are determined from the laboratory angular calibration of the spectrometer scans. These were normalized at the given wavelength of the resonance lines. Except for possible unknown systematic errors, these relative wavelengths are estimated to be accurate to .004 A for the O VII system and .002 A for Ne IX. The wavelengths derived for the I and S3 lines of Ne IX are in better agreement with the interpolated values from Flemberg's (1942) data than previous values which are summarized by Parkinson (1971) and Walker and Rugge (1970). The derived wavelengths are in excellent agreement with the recent theoretical work of Gabriel (1972) when the Ne IX wavelength scale is re-normalized to his resonance line wavelength.

According to the theory of Gabriel (1972), the upper level of the S3 satellite line is formed by dielectronic recombination and the strength of this line relative to the resonance line decreases approximately as the

inverse square of the electron temperature for the range of temperatures encountered in Table III. We have scaled S3/R ratios from Gabriel's theoretical curves for O VII and Ne IX at temperatures corresponding to the mean emission temperatures of Table III. Weighted averages of these S3/R ratios were computed with weights assigned according to the relative counts recorded from each region as given in Table I (listed general corona counts were multiplied by 20 to include the entire hemisphere). These average S3/R ratios may be compared directly with the experimental values of Table IV which are derived from the integrated spectra of Figure 8. The computed ratios are 0.025 and 0.08 for O VII and Ne IX respectively. Such precise agreement with the observed ratios is fortuitous but lends credence to Gabriel's theory.

The S3/R ratios averaged as above using the isothermal temperatures from Table II are 0.018 for O VII and 0.115 for Ne IX. Thus, agreement with the observations is poorer in the case of isothermal model and for Ne IX this disagreement is larger than our estimated experimental error.

The work of Gabriel and Jordan (1969) demonstrated that the ratio, R, of the intensities of the forbidden (F) to the intersystem (I) lines of helium-like ions is sensitive to electron density for sufficiently high densities. More recently, Freeman et al. (1971) and Blumenthal et al. (1971) have reconsidered the problem.

The values of R derived from our data for different coronal features are given in Table I and indicated in Figure 4. We have concluded earlier (Acton et al., 1971b) on the basis of these data that the absence of statistically significant variations among the R values implies that all regions observed are below the low density limit of 6×10^9 cm^{-3} given by Freeman et al. (1971). It is worth re-examining these data in view of the work of Blumenthal et al. (1971) which explicitely includes temperature dependent effects.

For the case in which the radiative excitation of the $1s2p\ ^3P$ levels from $1s2s\ ^3S_1$ is negligible, the dependence of the electron density, N_e,

on R may be conveniently written:

$$N_e = N_c \left((R_o/R) - 1 \right) \quad cm^{-3}. \qquad (7)$$

Blumenthal et al. (1971) give curves of R_o and N_c versus temperature for O VII. Their predicted variation of R_o, the low density limit of R, for the 1 - 2 x 10^6 K range is reproduced as a solid line in Figure 9. Over this range their value of N_c is approximately constant at 3.4 x 10^{10} cm^{-3}. Also plotted in Figure 9 are the R values from Table I versus the mean temperature of O VII line formation from Table III. Although the experimental accuracy is limited, the experimental R values tend to follow the trend of the R_o curve but fall systematically below it. For the apparent decrease of R below R_o of about five percent equation (7) indicates that the electron density within the O VII line forming portions of the active regions is of the order of 2 x 10^9 cm^{-3}.

The values of the parameter G, the ratio of forbidden plus intersystem lines to the resonance line, for the data of Figure 8 are 0.92 ± .01 and 0.90 ± .02 for O VII and Ne IX respectively. Corrections have been applied for the S4 satellite line under the assumption that it is equal in strength to S3 (Gabriel, 1972). The quoted errors are purely statistical.

6. Summary and Conclusions

The results of this rocket experiment show that much of the X-ray line emission from the solar corona may be unambiguously associated with corona overlying calcium plages. After the radiation from these compact regions has been accounted for, there remains a residual signal which is attributed to diffuse emission from above old plages and from the general corona. The compactness and contrast of the coronal sources increase with increasing energy. In this regard the coronal structures inferred from our monochromatic measurements are consistent with those seen on heterochromatic X-ray photographs obtained with high-resolution imaging systems. (Van Speybroeck et al. 1970.)

The changing geometry of the source regions with photon energy as well as the X-ray spectrometry of Batstone et al. (1970) indicate a need to go beyond a simple isothermal model in the interpretation of line ratio data. On the basis of an assumed emission measure distribution which varies as an inverse exponential with electron temperature, the following characteristics of the coronal plasma have been derived.

1) The decrease of the emission measure with temperature is 2 to 3 times as steep in the general corona as it is over active regions. Furthermore, the decrease of emission measure with temperature in a small dynamic feature is only one-half as steep as in the quiescent active regions.
2) Although there is a spread in T_o among the active regions, they seem to cluster around a value giving a tenfold decrease in emission measure for a 1.4×10^6 K increase in temperature. This fact, when considered with the small signal observed from these regions by the proportional counter spectrometer, is not compatible with the results of Batstone et al. (1970). We conclude that the three active regions which they describe are all higher energy features.
3) Under the assumption of spherical symmetry, we find the RMS electron density in the general corona is of the order of 4×10^8 cm^{-3}. The total emission measure of the coronal hemisphere above 10^6 K is about 2×10^{49} cm^{-3}. This value is in agreement with that derived by Elwert (1954) on the basis of the Baumbach model of the quiet corona.
4) The active regions contribute about one-third of the total coronal emission measure but less than five percent of the total coronal material.

We find that the trend with temperature of the ratio, R, of the forbidden to intersystem lines for O VII agrees with the work of Blumenthal et al. (1971). Although it is at the limit of our experimental accuracy, the apparent systematic departure of R below Blumenthal's R_o may be interpreted as indicating densities of the order of 2×10^9 cm^{-3} in the O VII

emitting portions of active regions. This electron density with the total emission measures of Table III indicate emitting volumes of the order of 4×10^{29} cm^3 for characteristic dimensions of 2 arcmin. This is consistent with the data of Figure 4a which show the O VII sources to be somewhat extended compared to the 1.7 arcmin field of view.

Comparison of the S3 satellite to resonance line ratios from our integrated O VII and Ne IX spectra with suitably averaged theoretical values from Gabriel's (1972) work relating satellite line strength to dielectronic recombination shows good agreement for data reduced on the basis of the non-isothermal model which we have used. Discordant results are obtained when the comparison is based on data reduced according to an isothermal approximation.

Wavelengths have been assigned to the principal emission lines in the 13.34 - 13.78 and 21.38 - 22.27 A ranges based on the angular scan calibration of our Bragg spectrometers. In general, these wavelengths agree well with previous results (Walker and Rugge, 1970; Parkinson, 1971). Wavelengths for the intersystem and one of the satellite lines of Ne IX are in better agreement with interpolared predictions than previous results.

ACKNOWLEDGEMENTS

This work has been supported by the National Aeronautics and Space Administration under contracts NASw-1834 and NAS2-6723 and by the Lockheed Independent Research Program. We are indebted to the following institutions for their ground-based support of our experiment: Aerospace Corporation, Big Bear Solar Observatory, Lockheed Solar Observatory, Mauna Loa Observatory, Mees Solar Laboratory, Sacramento Peak Observatory and the Space Environment Services Center in Boulder. We wish to thank Dr. Alan H. Gabriel of Culham Laboratory for the use of his materials in advance of publication.

R. Caravalho, C.W. Gilbreth, A.S. Knapp, D.T. Roethig, and K.L. Smith of Lockheed made important technical contributions to the project. We acknowledge the

excellent technical support provided by Ames Research Laboratory, Vehicle Guidance and Control Branch (SPARCS, vehicle instrumentation), and Goddard Space Flight Center Sounding Rocket Division (vehicle support) and the launch and range and recovery support coordinated by Mr. Lloyd Briggs at White Sands Missile Range.

L.W. Acton enjoyed the hospitality of the Arbeitsgruppe fur Physikalische Weltraumforschung in Freiburg, Germany, during the preparation of this paper.

REFERENCES

Acton, L.W., Catura, R.C., Culhane, J.L., and Meyerott, A.J.: 1971a, in New Techniques in Space Astronomy (ed. by Labuhn and Lust), D. Reidel Publ. Co., Dordrecht, p. 181.

Acton, L.W., Catura, R.C., Meyerott, A.J., and Culhane, J.L.: 1971b, Nature, 233.

Batstone, R.M., Evans, K., Parkinson, J.H., and Pounds, K.A.: 1970, Solar Phys., 13, 389.

Blumenthal, G.R., Drake, G.W.F., and Tucker, W.H.: 1971, Astrophys. J., 172, 205.

Catura, R.C., Acton, L.W., Culhane, J.L. and Meyerott, A.J.: 1972, presented at the Third Symposium of Ultraviolet and X-ray Spectroscopy of Astrophysical and Laboratory Plasmas, Utrecht, August 1971, (Summary to be published in Space Science Review).

Chambe, G.: 1971, Astron. Astrophys., 12, 210.

Charles, M.W.: 1968, Thesis, University of Leicester, Leicester, England.

Compton, A.H., and Allison, S.K.: 1935, X-Rays in Theory and Experiment, D. Van Nostrand Co., Inc., Princeton.

Elwert, G.: 1954, Zs. f. Natursorsch, 9a, 637.

Evans, K. and Pounds, K.A.: 1968, Astrophys. J., 152, 319.

Flemberg, H.: 1942, Ark. Mat. Astron. Fys., 28A, 1.

Freeman, F.F., Gabriel, A.H., Jones, B.B. and Jordan, C.: 1971, Phil. Trans. Roy.Soc. Series A, 270, 127.

Gabriel, A.H.: 1972, submitted for publication to Monthly Notices Roy. Astron. Soc..

Gabriel, A.H. and Jordan, C.: 1969, Monthly Notices Roy. Astron. Soc., 151, 141.

Jordan, C.: 1966 Monthly Notices Roy. Astron. Soc., 132, 463.

Jordan, C.: 1969 Monthly Notices Roy. Astron. Soc., 142, 501.

Liefeld, R.J.,Hanzely, S., Kirby, T.B., and Mott, D.: 1970, Adv. in X-Ray Analysis, 13, 378.

Parkinson, J.H.: 1971, Thesis, University of Leicester, Leicester, England.

Rugge, H.R. and Walker, A.B.C.: 1970, Solar Phys., 15, 372.

Rugge, H.R. and Walker, A.B.C.: 1971, Solar Phys., 18, 244.

Schweizer, W., and Schmidtke, G.: 1971, Astrophys. J. Letters, 169, L27.

Seaton, M.J.: 1964 Planet. Space Sci., 12, 55.

Van Regemorter, H.: 1962, Astrophys. J., 136, 906.

Van Speybroeck, L.P., Frieger, A.S., and Vaiana, G.S.: 1970, Nature, 227, 818.

Walker, A.B.C., and Rugge, H.R.: 1970, Astron. Astrophys., 5, 4.

Widing, K.G. and Sandlin, G.D.: 1968, Astrophys. J., 152, 545.

Withbroe, G.: 1971, Solar Phys., 18, 458.

Table I

EXPERIMENTAL DATA

Plage Region	Counts* O VII	Counts* Ne IX	O/Ne** Ratio	R† O VII	R† Ne IX
289	672 ± 146	605 ± 43	1.11 ±.25	3.7 ±.1	3.1 ± .1
279, 274B	400 ± 73	214 ± 33	1.87 ±.45	3.7 ±.1	3.2 ± .2
281	365 ± 44	148 ± 17	2.47 ±.41	3.6 ±.1	2.8 ± .2
274A	473 ± 128	148 ± 43	3.20 ±1.27	3.4 ±.15	2.9 ± .2
286	492 ± 73	142 ± 30	3.46 ±.89	3.5 ±.1	3.3 ± .2
265,266	427 ± 47	92 ± 10	4.65 ±.72	3.7 ±.2	3.0 ± .3
Gen.Corona	225 ± 5	21 ± 1	10.71 ±.56	3.4 ±.1	2.9 ± .2

* Counts in the resonance line ($1s^2\ ^1S_o$ - $1s2p\ ^1P_1$) normalized to one crystal rotation and best collimator aspect.

** Ratio of counts recorded in the two resonance lines.

† Ratio of forbidden ($1s^2\ ^1S_o$ - $1s2s\ ^3S_1$) to intersystem ($1s^2\ ^1S_o$ - $1s2p\ ^3P$) line intensities.

TABLE II

ISOTHERMAL MODEL

Plage Region	Electron Temperature (10^6 K)	Emission Measure (10^{47} cm^{-3})
289	2.40	16
279, 274B	2.15	8
281	2.05	7
274A	1.95	9
286	1.90	9
265, 266	1.80	8
Gen. Corona	1.45	140*

* Emission measure of coronal hemisphere facing the earth.

TABLE III

NON-ISOTHERMAL (EXPONENTIAL) MODEL

Plage Region	T_o (10^6 K)	C*	EM_{tot} ** (10^{47} cm^{-3})	$\langle T_{O\ VII} \rangle$ (10^6 K)	$\langle T_{Ne\ IX} \rangle$ (10^6 K)	$EM_{Ne\ IX}$ (10^{47} cm^{-3})
289	3.15	3	23	1.95	3.10	13
279, 274B	1.80	6	13	1.80	2.70	5
281	1.50	8	12	1.70	2.55	4
274A	1.25	18	16	1.65	2.40	4
286	1.15	24	16	1.60	2.30	4
265, 266	0.95	42	15	1.50	2.20	3
Gen. Corona†	0.60	170	170	1.25	1.70	10

* The constant of equation (4). Units: 10^{48} cm^{-3} (10^6 K)$^{-1}$.

** Emission measure above 10^6K. Essentially equal to O VII emission measure.

† All values refer to coronal hemisphere facing the earth.

TABLE IV

SPECTRA

Line (Fig. 9)	Transition	λ - O VII (A)	Relative Strength** This Work	*	λ - Ne IX (A)	Relative Strength** This Work	*
R	$1s^2\ {}^1S_o - 1s2p\ {}^1P_1$	21.602			13.447		
S1		21.642*	≤ .04		13.469*	~ .06	.016
S2		21.677*			13.488*		.012
I	$1s^2\ {}^1S_o - 1s2p\ {}^3P_{1,2}$	21.805			13.551		
S3	$1s^2 2s\ {}^2S^e - 1s2p2s\ {}^2P^o$	22.024	~ .025	< .04	13.651	~ .09	~ .04
F	$1s^2\ {}^1S_o - 1s2s\ {}^3S_1$	22.103			13.700		
S4	$1s^2 2p\ {}^2P^o - 1s2p2p\ {}^2D^e$	22.108*			13.703*		

* Parkinson (1971)

** Strength of satellite line(s) relative to resonance line.

FIGURE CAPTIONS

Figure 1. A schematic view of the primary instrumentation in the rocket payload.

Figure 2. A solar disc photograph in H-alpha taken near the time of flight by the Lockheed Solar Observatory. The scan directions and the field of view of the crystal spectrometers are indicated on the photograph.

Figure 3. O VII and Ne IX spectra of McMath plage No. 281 accumulated during flight in approximately five seconds. Resonance, intersystem and forbidden transitons are labelled R, I and F respectively.

Figure 4. Plots of the total line emission and the forbidden to intersystem line ratio (R) from O VII (a) and Ne IX (b) acquired during the first scan across the disc. The continuum near 3 A (3-7 keV) obtained by the Be-window counter during this scan is shown in (c). The solid lines indicate the triangular shaped collimator response which has been fitted to the active region emissions with the McMath-Hulbert Plage numbers of each region resolved shown above the triangles. Contribution of the general corona, extrapolated over the disc as described in the text is shown by the small squares in part (a). The data gap at plus 10 arcmin was caused by a momentary malfunction of the attitude control system.

Figure 5. Plots of total line emission against disc position for Ne IX (a) and 3-7 keV continuum (b) taken from the second rocket scan. Contribution from each active region is indicated by the McMath-Hulbert numbers above each triangle.

Figure 6. The location of X-ray emitting regions on the disc are shown together with an H-alpha photograph. The McMath-Hulbert plage map is for the day before the flight.

Figure 7. The ratio of O VII to Ne IX resonance line counts plotted against electron temperature for an isothermal model (a) and against the

parameter T_o of equation (4) for a model (b) in which the emission measure decreases exponentially with a slope determined by T_o.

Figure 8. Spectra summed to include all useful data from both scans of the disc but excluding the flaring region (plage 289). Position of reported satellite lines are indicated by S1-S4. Line widths of the Ne IX lines are determined by the collimation while those of O VII are essentially the rocking curve of the KAP crystal. Intersystem line of Ne IX is broadened relative to R or F lines by the fine structure of this transition or because of an unreported blend. The double width steps seen at 13.47 and 13.69 in the Ne IX spectra are caused by the treatment of these data in the flight data processor and not by errors in the crystal scan.

Figure 9. The solid curve is the forbidden to intersystem line ratio in the low density limit (R_o) taken from Blumenthal et al. (1971). It is plotted versus the electron temperature of the line forming region. The experimental data points are the O VII R values for the coronal regions listed in Table I. In this case, the abcissa is $< T_{O\ VII} >$, the corresponding mean emission temperatures from Table III.

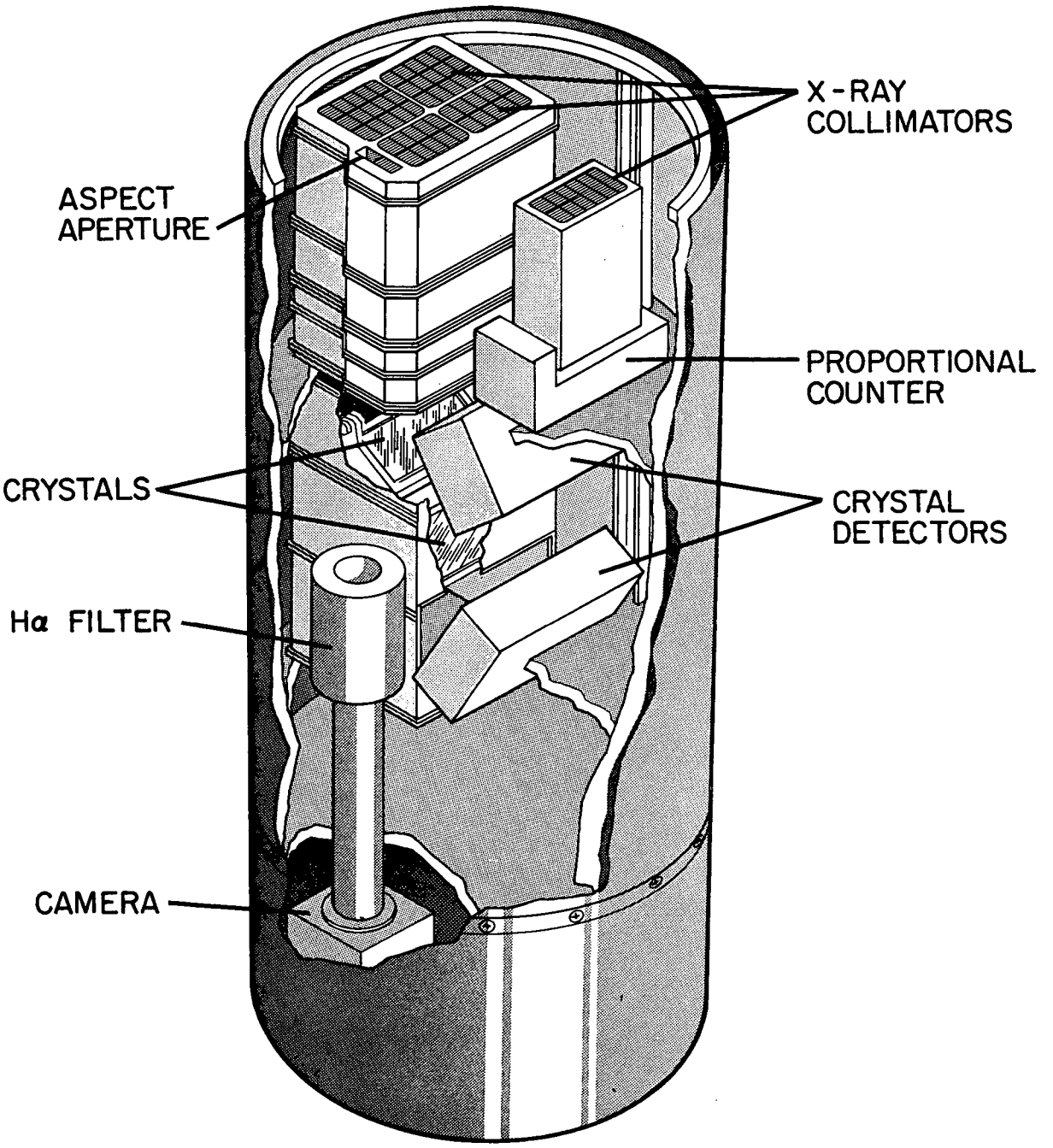
X-RAY
COLLIMATORS
ASPECT
APERTURE
PROPORTIONAL
COUNTER
CRYSTALS
CRYSTAL
DETECTORS
Hα FILTER
CAMERA

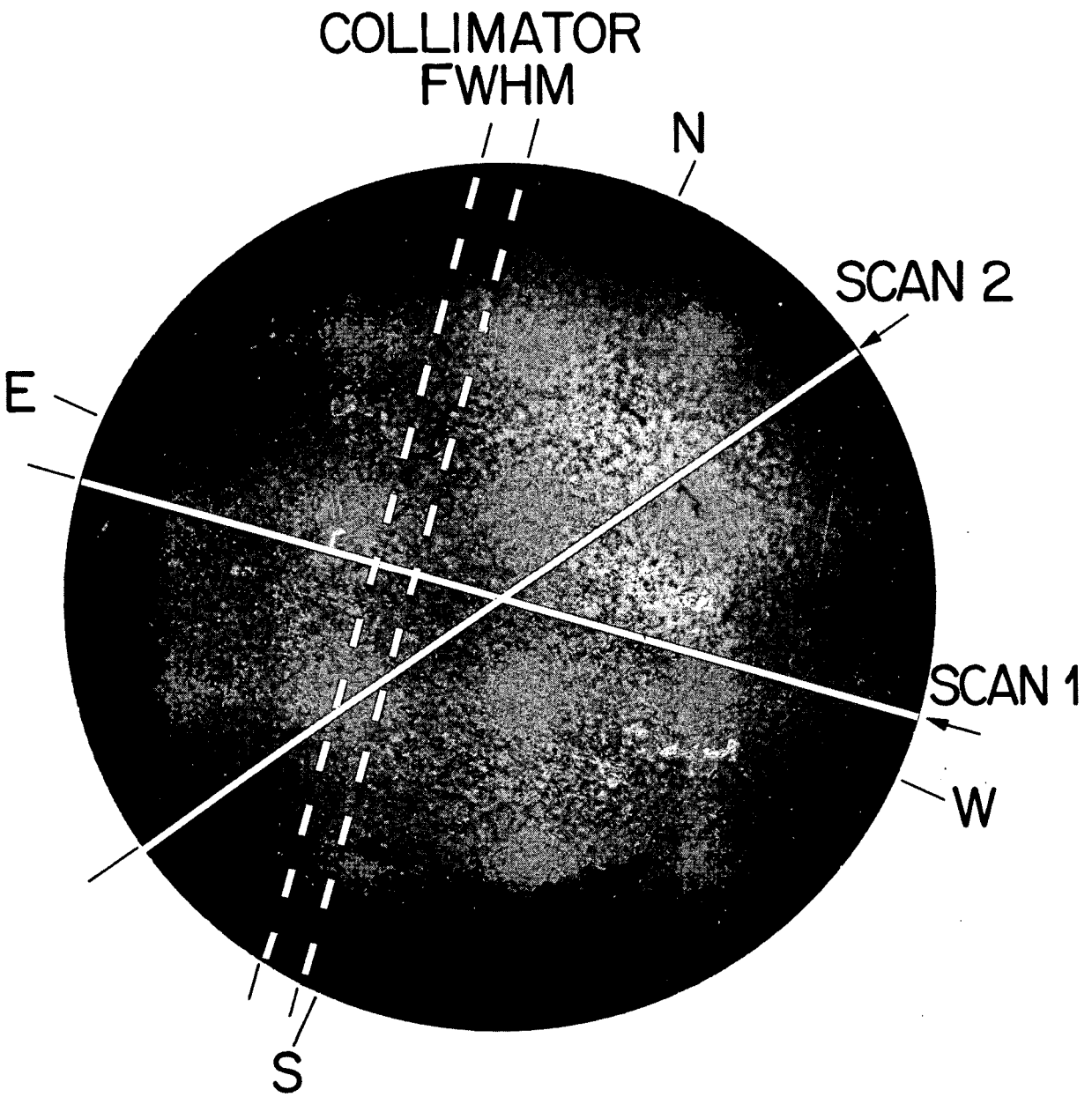

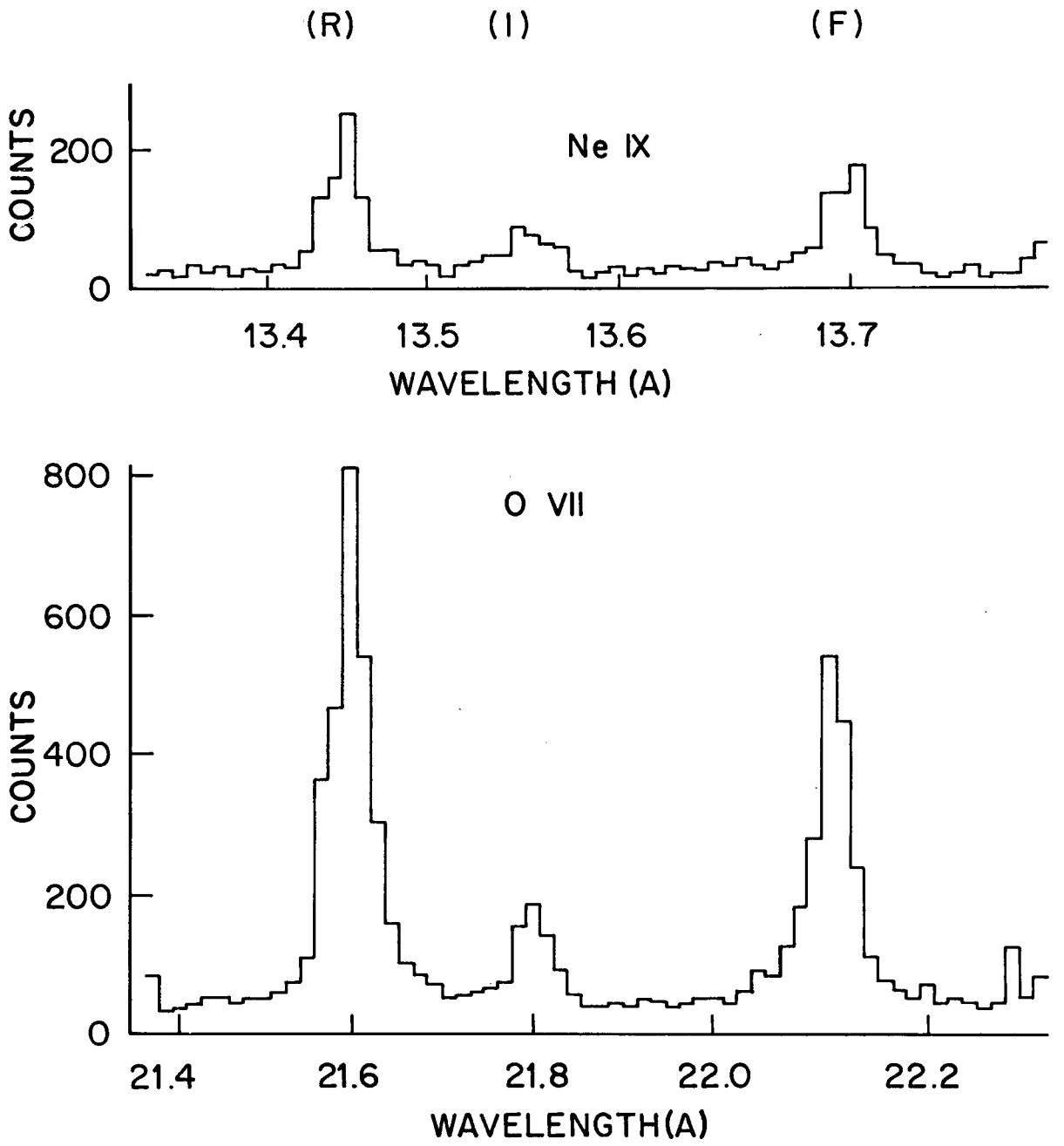
(R)
(I)
(F)
Ne IX
COUNTS
200
0
13.4
13.5
13.6
13.7
WAVELENGTH (A)
O VII
800
600
400
200
0
21.4
21.6
21.8
22.0
22.2
WAVELENGTH(A)

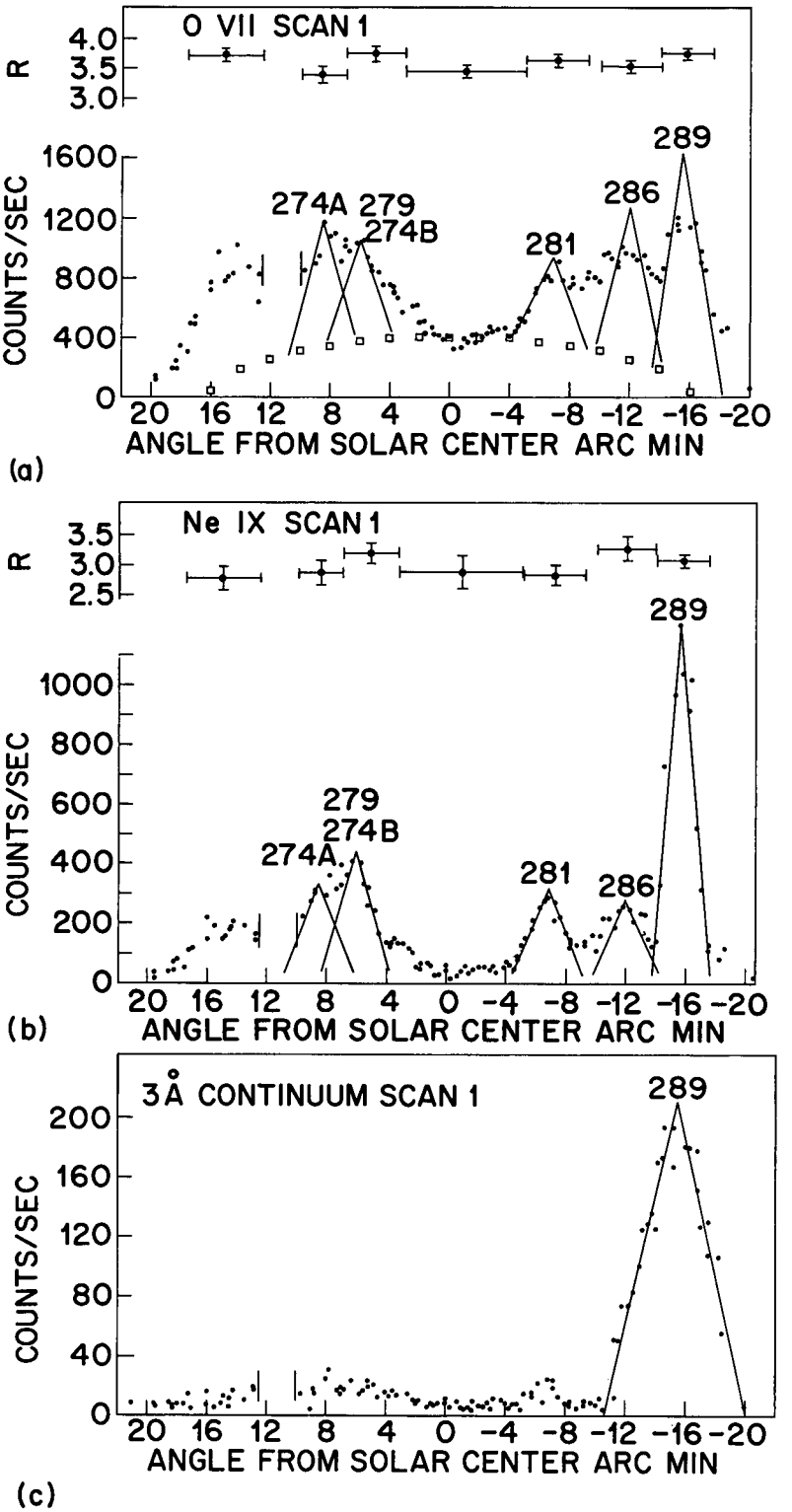
O VII SCAN 1
R
4.0
3.5
3.0
1600
1200
800
400
0
COUNTS/SEC
274A
279
274B
281
286
289
20 16 12 8 4 0 -4 -8 -12 -16 -20
ANGLE FROM SOLAR CENTER ARC MIN
(a)
Ne IX SCAN 1
R
3.5
3.0
2.5
1000
800
600
400
200
0
COUNTS/SEC
279
274B
274A
281
286
289
20 16 12 8 4 0 -4 -8 -12 -16 -20
ANGLE FROM SOLAR CENTER ARC MIN
(b)
3Å CONTINUUM SCAN 1
200
160
120
80
40
0
COUNTS/SEC
289
20 16 12 8 4 0 -4 -8 -12 -16 -20
ANGLE FROM SOLAR CENTER ARC MIN
(c)

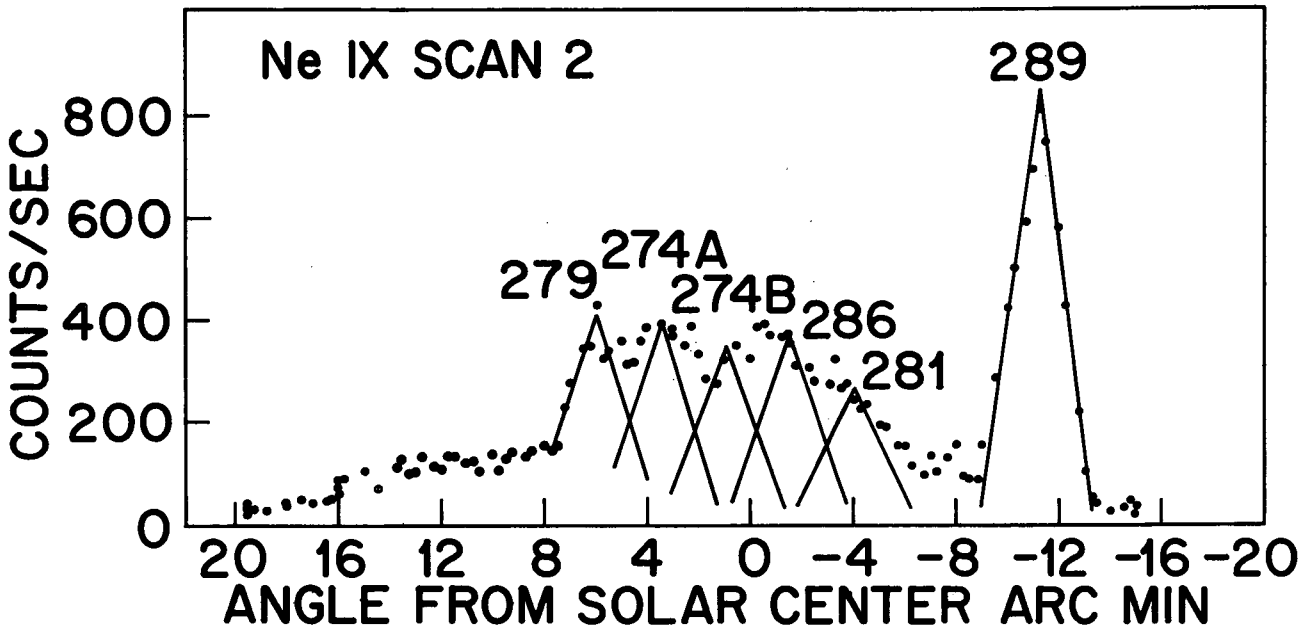
Ne IX SCAN 2
289
279
274A
274B
286
281
COUNTS/SEC
800
600
400
200
0
20 16 12 8 4 0 -4 -8 -12 -16 -20
ANGLE FROM SOLAR CENTER ARC MIN

(a)

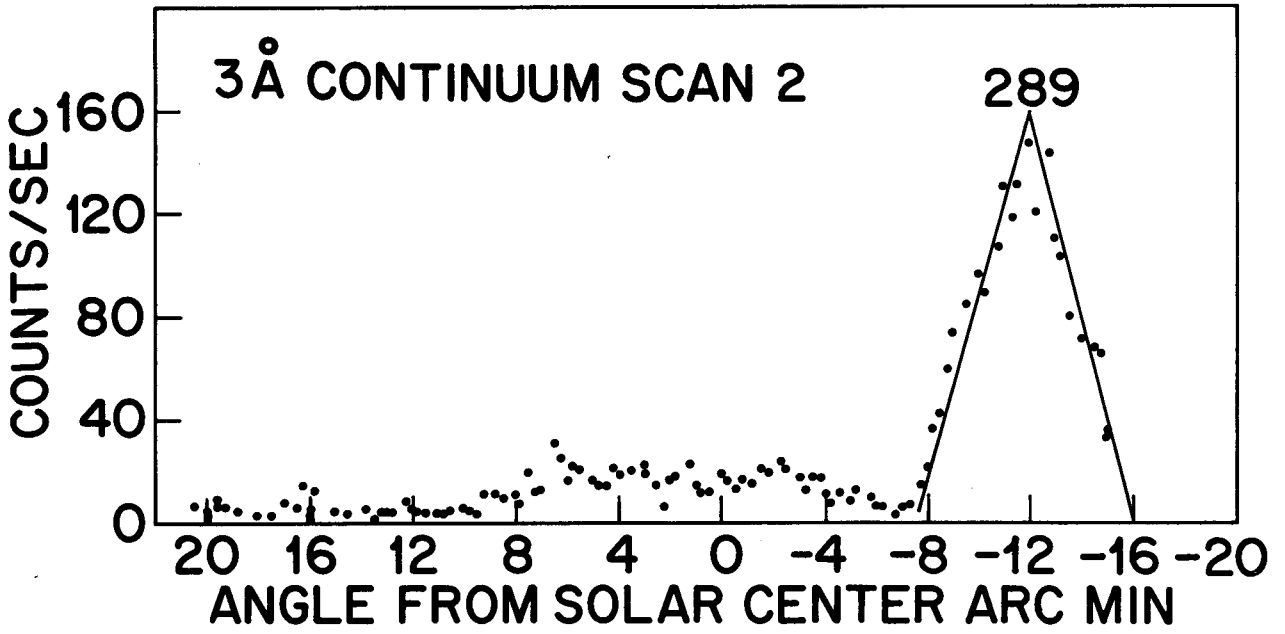
3Å CONTINUUM SCAN 2
289
COUNTS/SEC
160
120
80
40
0
20 16 12 8 4 0 -4 -8 -12 -16 -20
ANGLE FROM SOLAR CENTER ARC MIN

(b)

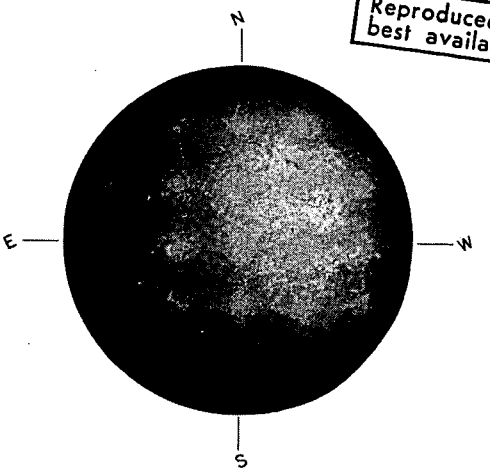

McMATH-HULBERT CALCIUM REPORT

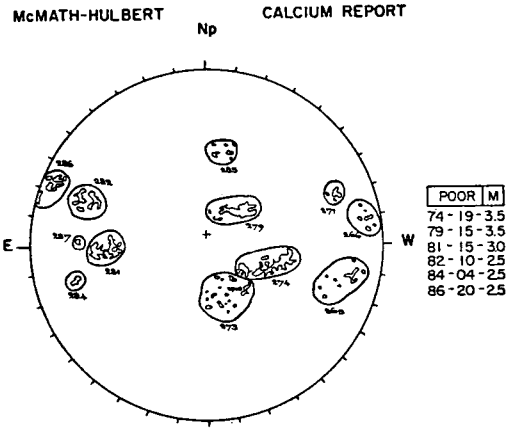

1500 UT

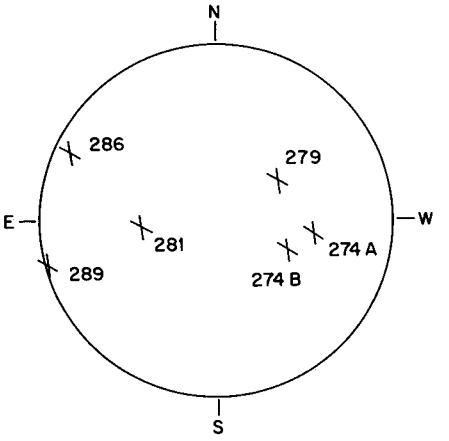

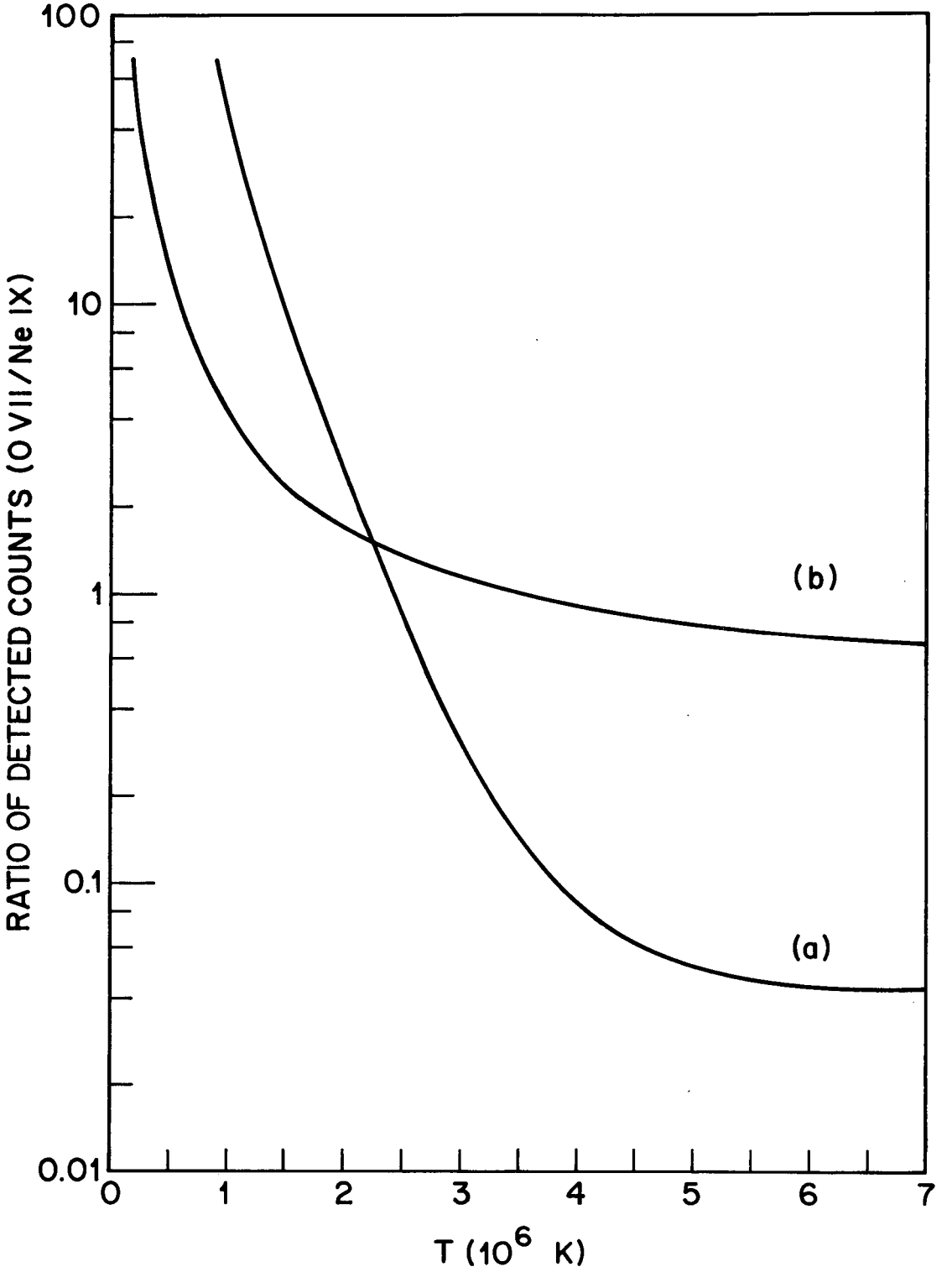
100
10
1
0.1
0.01
RATIO OF DETECTED COUNTS (O VII / Ne IX)
(b)
(a)
0
1
2
3
4
5
6
7
T (10^6 K)

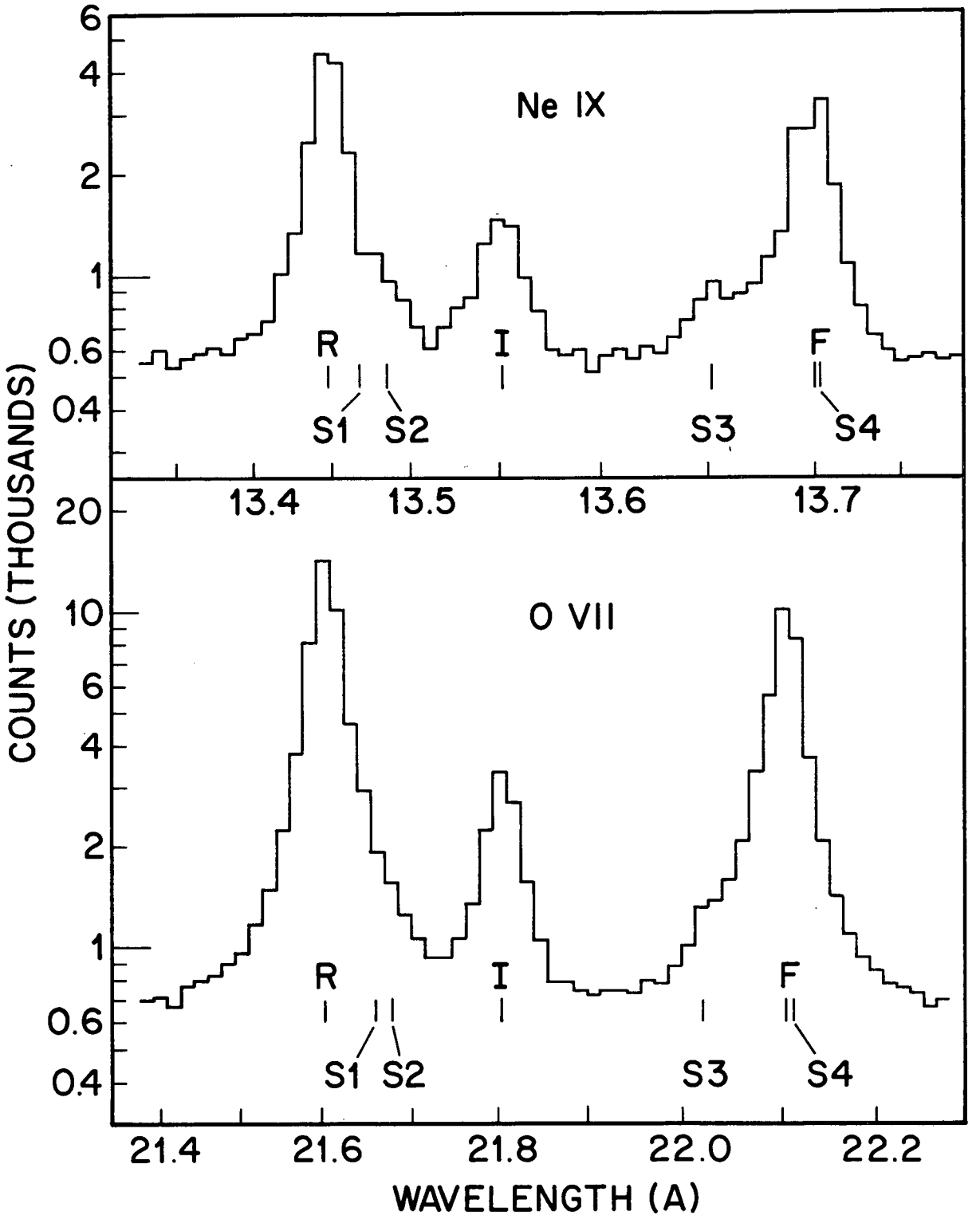
Ne IX
R
I
F
S1
S2
S3
S4
13.4
13.5
13.6
13.7
O VII
R
I
F
S1
S2
S3
S4
21.4
21.6
21.8
22.0
22.2
WAVELENGTH (A)
COUNTS (THOUSANDS)
6
4
2
1
0.6
0.4
20
10
6
4
2
1
0.6
0.4

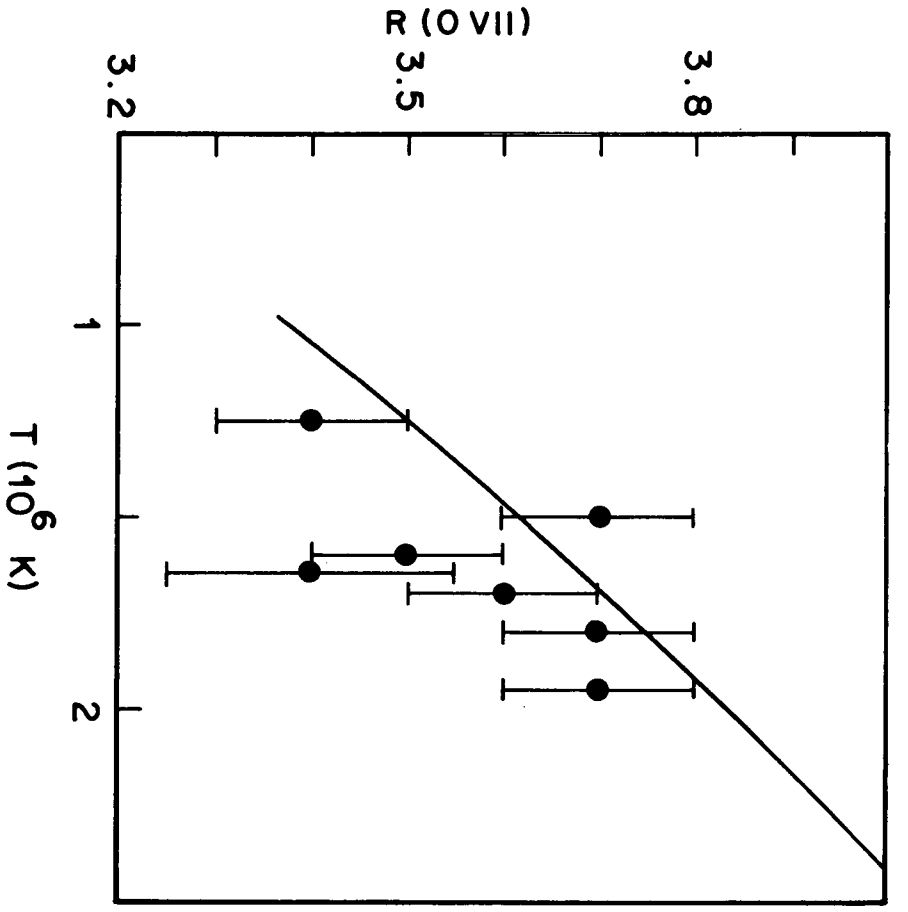
R (O VII)
3.2
3.5
3.8
1
2
T (10^6 K)

APPENDIX 5

X-RAY STUDY OF SOLAR PLAGE REGIONS AND A SMALL FLARE

L. W. Acton, R. C. Catura

Lockheed Palo Alto Research Laboratory, Palo Alto, California, USA

and J. L. Culhane

University College London, Mullard Space Science Laboratory,

Holmbury St. Mary, Dorking, Surrey, England

Abstract

The O VII and Ne IX resonance line and 5 keV continuum emission of a small solar flare are interpreted on the basis of a model in which the emission measure of the region is an exponentially decreasing function of temperature. Good agreement with all three sets of data is obtained--a result not possible on the basis of an isothermal approximation. The change in the emission of the flare over a two minute interval appears to be consistent with a simple cooling of the region. Computation of the contribution function versus temperature for each emission indicates that each predominantly comes from a physically separate volume within the feature. The emission measure distribution for the flare is distinctly flatter than that of five plage regions which tend to have similar slopes and which are in turn flatter than the general corona.

To be published in SPACE RESEARCH XIII

1. Introduction

Measurement of the x-ray line and continuum emission from the sun can provide basic information on the physical state of the coronal plasma. Such a study was the object of a rocket experiment, flown 29 April 1971 from White Sands Missile Range, New Mexico, which provided sufficient spectral and spatial resolution to permit the observation of the resonance line emission from the helium-like ions O VII (21.6 A) and Ne IX (13.4 A) from the general corona, five quiescent plage regions and the late stages of a small flare. These emission line data have been interpreted on the basis of a simple non-isothermal model and published, along with a description of the experiment and instrumentation, by Acton, Catura, Meyerott, Wolfson and Culhane [1]. In the present paper we extend that work, further analyzing the flare data to take into account the observed 5 keV continuum.

2. Data Analysis

The rocket payload included two collimated plane Bragg spectrometers using large (97 cm^2 each) KAP crystals to cover the wavelength ranges 21.4 - 22.3 A for O VII and 13.3 - 13.8 A for Ne IX, a collimated proportional counter spectrometer covering the nominal energy range 4 - 15 keV, an optical aspect camera operating at 6563 A (H-alpha) with a 1 A filter, and a photographic EUV spectrograph provided by the Arbeitsgruppe für Physikalische Weltraumforschung, Freiburg, Federal Republic of Germany.

The Oda-type collimators of the crystal spectrometers defined a field of view 1.7 arcmin wide (FWHM) in the direction of dispersion.

The field of view of the proportional counter spectrometer was 4.2 arcmin FWHM in the narrow dimension and was aligned with the field of view of the crystal spectrometers. During the data-gathering portion of the rocket flight these fan beam fields of view were swept across the sun at an angular rate of about 0.3 arcmin/sec under the control of the SPARCS attitude control system. After completing one transit of the sun the rocket was rolled 130° to reorient the fields of view and a second slow scan of the disk was accomplished.

Figure 1 illustrates the data from the three spectrometers for the first transit of the sun. The numbers given on the figure are the McMath plage numbers of the different regions. We are primarily concerned with region 289 in which a small flare (-N) with accompanying surge had taken place about 15 minutes before launch -- but without reported impulsive x-ray or radio events. The angular profile of region 289 in Figure 1 has been broadened by a small pointing control oscillation. However, all evidence indicates that this source region is small compared with our 1.7 arcmin field of view.

As the x-ray emissivity of an element of volume is proportional to the square of the electron density it is the usual practice to analyze x-ray data in terms of the emission measure--the integral of the square of the electron density over the source volume--of the source. Thus, in the common isothermal approximation the parameters which are determined are an electron temperature and an emission measure for the source.

It is not possible to simultaneously account for the intensity of the O VII and Ne IX emission lines and the strength of the 5 keV

continuum from region 289 of Figure 1 on the basis of an isothermal approximation. The line and continuum data would require source temperatures of 2.4 and 7 million K respectively. Since it is reasonable to assume that any real coronal source region will exhibit a range of temperatures, we have analyzed these data on the basis of a model proposed by Chambe [2] in which the emission measure is an exponentially decreasing function of the electron temperature. Specifically,

$$M(T) = \frac{d}{dT} \int N^2 \, dV = C \, 10^{-T/Q} \ \ cm^{-3} \ (10^6 \ K)^{-1} \qquad (1)$$

is the differential emission measure. T is the electron temperature, N is the electron density, C is a constant and Q is a parameter with the dimensions of a temperature which specifies the slope of the emission measure distribution. This formalism has the advantage that it fits our data reasonably well and at the same time provides a convenient form for computing mean plasma parameters.

3. Results

Using this technique with the O VII and Ne IX emission line data we had earlier determined [1] that for region 289 the parameter Q lies within the range 4.3 - 2.5 x 10^6 K and the parameter C is approximately equal to 3 x 10^{48} cm^{-3} $(10^6 \ K)^{-1}$. The large uncertainty in Q reflects the relatively large error in the O VII data for this source.

Under the assumption that the x-rays detected around 5 keV are a bremsstrahlung continuum from a source with a helium abundance of about 0.2 and unit Gaunt factor we have computed the signal to be

expected from our proportional counter spectrometer as a function of the parameters C and Q of equation 1. For this analysis we have used the data in the 4.5 - 5.9 keV channel of the pulse height analyzer (effective energy 5.1 keV) as we believe these data to be the most reliable.

For the decaying flare in region 289 we derive the following values for the parameters of equation 1 from the observed strength of the Ne IX resonance line and 5 keV continuum.

$$Q = 2.8 \pm 0.1 \times 10^{6} \text{ K}$$
$$C = 4.5 \times 10^{48} \text{ cm}^{-3} (10^{6} \text{ K})^{-1}. \qquad (2)$$

This solution is compatible with our O VII resonance line data. In Figure 2 we compare this differential emission measure distribution (curve F) with the distributions given in reference [1] for five quiescent plage regions (curves P) and the general corona (curve C). The curve for the quiet corona has been normalized to one coronal hemisphere based on a spherically symmetric model.

Figure 3 presents the relative contribution to the O VII, the Ne IX and the 5 keV continuum emission from the different temperature regimes for the differential emission measure distribution of the flare. These curves demonstrate that even within the relatively compact flare the bulk of each of these radiations predominantly comes from separate and distinct volumes. We have used the contribution functions of Figure 3 to compute the following mean emission temperatures and effective emission measures for the O VII, the Ne IX and the 5 keV regions:

O VII $\langle T \rangle = 1.9 \times 10^6$ K, EM = 1×10^{48} cm^{-3}.

Ne IX $\langle T \rangle = 3.0 \times 10^6$ K, EM = 5×10^{47} cm^{-3}.

5 keV $\langle T \rangle = 9.1 \times 10^6$ K, EM = 1×10^{46} cm^{-3}.

During the interval of 120 seconds between the first and second observation of region 289 the 5 keV flux decreased by about 30 percent and the Ne IX flux by some 20 percent. (We have no O VII data from the second transit because of a detector malfunction.) The resulting change of the slope parameter Q of the exponential emission measure distribution is a decrease from 2.8 to 2.7×10^6 K with no change of the amplitude parameter C. This result is also consistent with the pulse height spectra of our proportional counter spectrometer and probably represents a simple cooling of the post flare plasma.

4. Acknowledgments

This work has been supported by the National Aeronautics and Space Administration under contracts NASW-1834 and NAS2-6723 and by the Lockheed Independent Research Program. L. Acton has enjoyed the hospitality of the Arbeitsgruppe für Physikalische Weltraumforschung in Freiburg during the preparation of this paper.

5. References

[1] L. W. ACTON et al., Solar Phys. (to be published).

[2] G. CHAMBE, Astron. Astrophys 12, 210 (1971).

Figure Captions

Figure 1 Relative intensity in the three radiations observed on the first transit of the sun. The upper, center and lower curves are O VII, Ne IX and 3.2 - 7 keV continuum respectively. The small squares in the upper portion indicate the assumed general coronal signal.

Figure 2 Derived exponential emission measure distributions for the general corona (C), five quiescent plage regions (P) and the decaying -F solar flare (F).

Figure 3 The relative contribution to the O VII and Ne IX resonance lines and the 5 keV continuum as a function of temperature within the flare feature for an exponential emission measure distribution having a slope parameter, Q, of 2.8×10^6 K. The amplitudes of the three curves relative to one another is arbitrary.

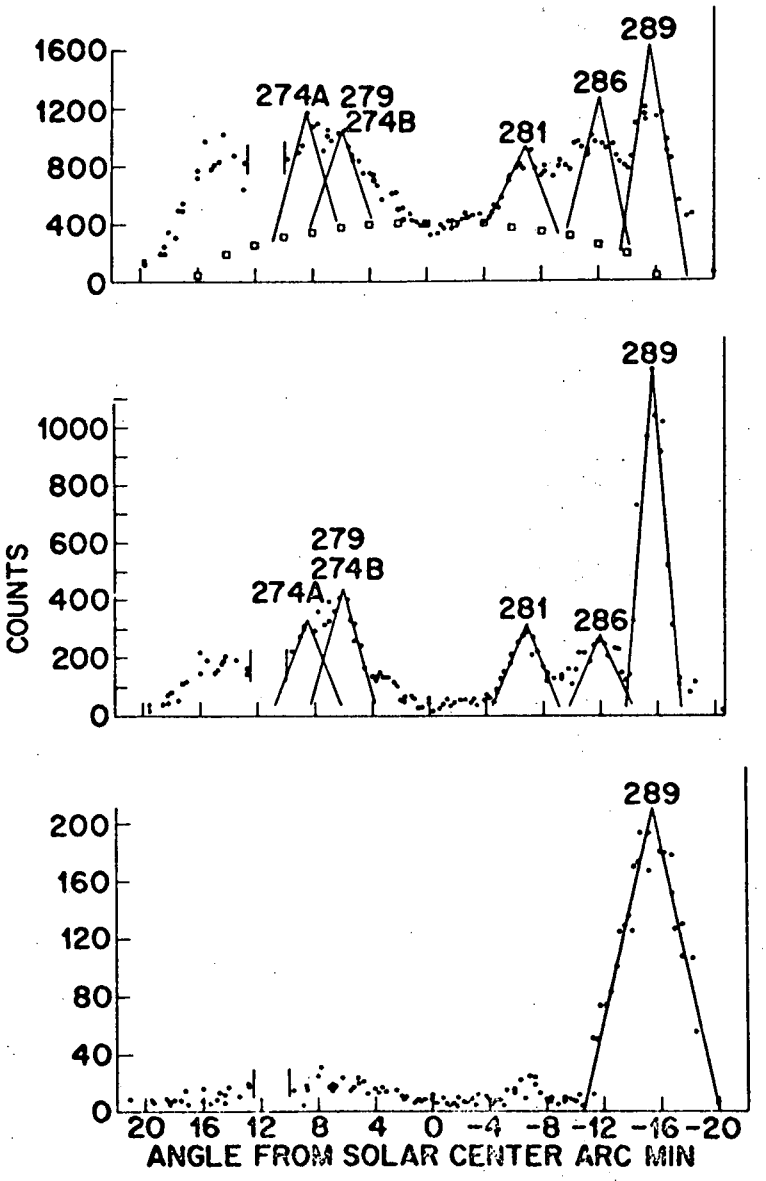
1600
1200
800
400
0
274A
279
274B
281
286
289
1000
800
600
400
200
0
COUNTS
279
274B
274A.
281
286
289
200
160
120
80
40
0
20 16 12 8 4 0 -4 -8 -12 -16 -20
ANGLE FROM SOLAR CENTER ARC MIN

Fig. 1

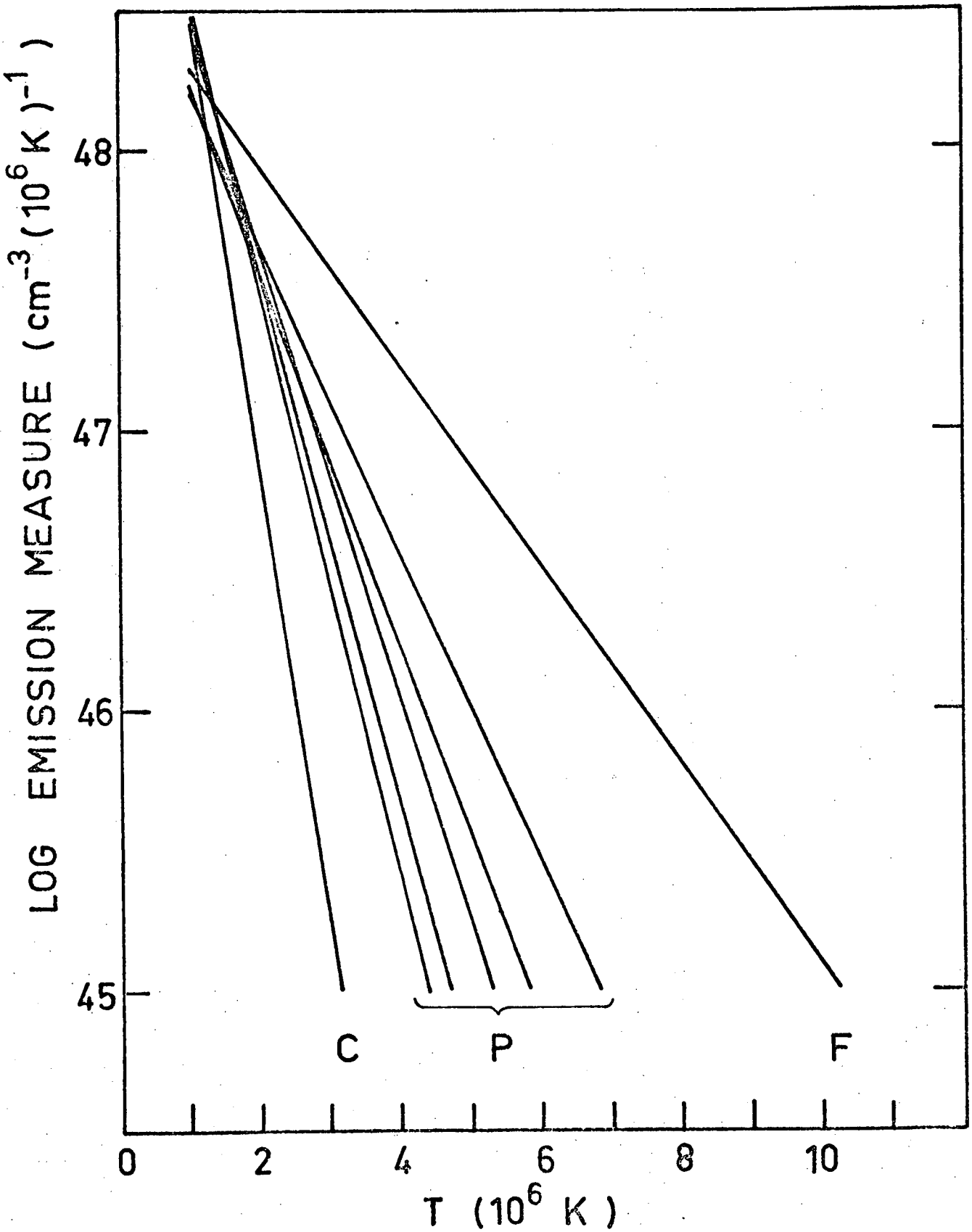

72

Fig. 2

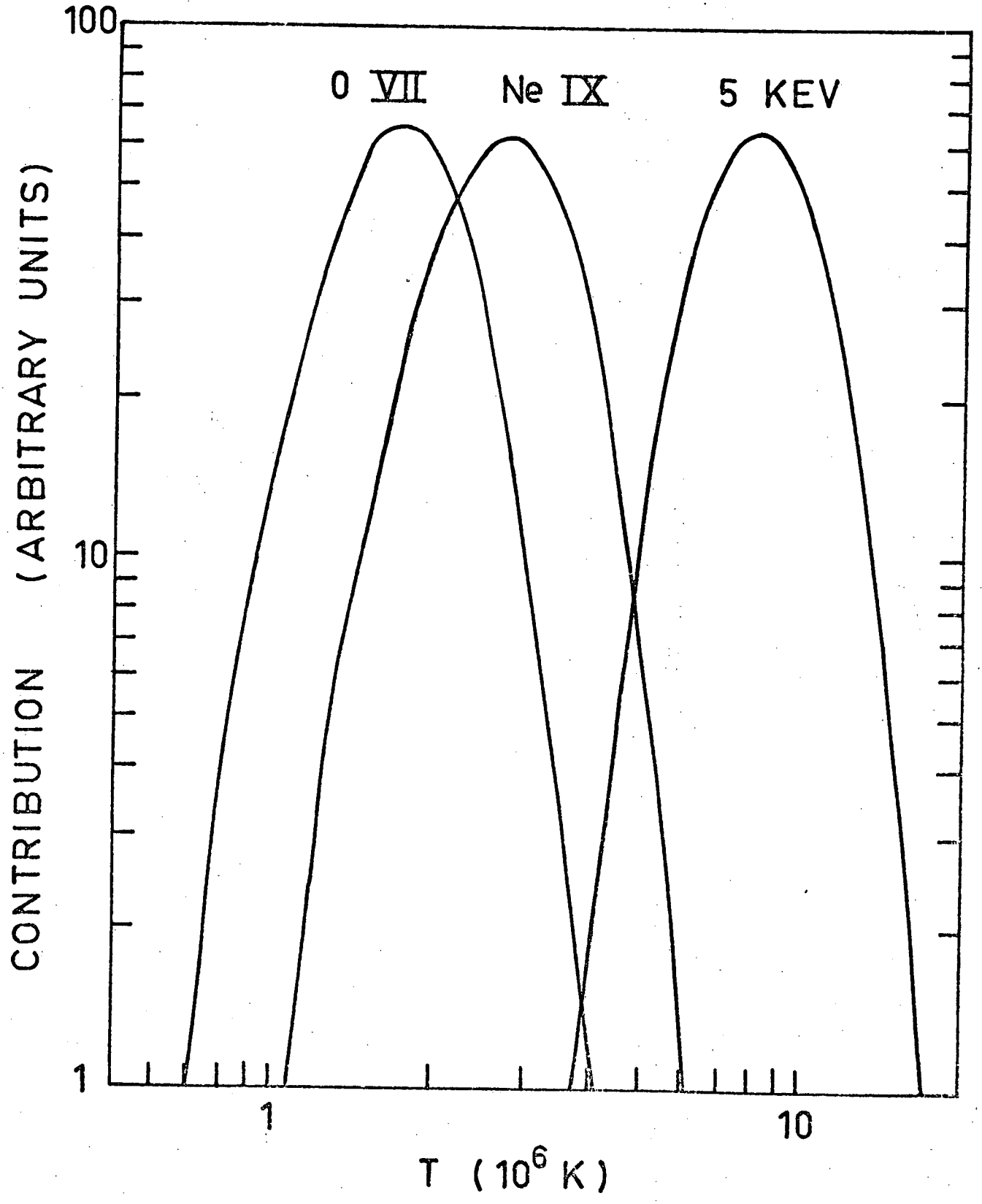
100
10
1
CONTRIBUTION (ARBITRARY UNITS)
O VII
Ne IX
5 KEV
1
10
T (10^6 K)

Fig. 3

APPENDIX 6

(Abstract of paper presented at a meeting of the Solar Physics Division of the American Astronomical Society at the University of Maryland on 3-5 April, 1972.)

Analysis of X-Ray Line Emission from Individual Solar Active Regions, R.C. CAIURA, L.W. ACTON, and C.J. WOLFSON, Lockheed Palo Alto Research Laboratory, and J.L. CULHANE, MSSL, University College London. - Selected X-ray lines of O VII and Ne IX emitted by the solar corona have been observed on a recent rocket flight by using collimated Bragg crystal spectrometers sensitive in the ranges21.4-22.3A and 13.3-13.8A. The principal lines observed result from the transitions ($2s^2\ {}^1S_0$- $1s2p\ {}^1P_1$), ($2s^2\ {}^1S_0$- $1s2p\ {}^3P$) and ($2s^2\ {}^1S_0$- $1s2s\ {}^3S_1$) in these He-like ions. The data have been spatially resolved into contributions from at least seven active regions and the general corona. Temperatures and emission measures for each of these sources have been calculated assuming the resonance line emission from each of the ions is due to an isothermal plasma. The resulting temperatures for the active regions range from 1.8 to 2.4 x 10^6K, while the value for the general corona is 1.5 x 10^6K. Values of active region emission measure are in the range from 7 to 16 x 10^{47} cm^{-3}. The total emission measure above 10^6K for one hemisphere of uniform general corona is 2 x 10^{48} cm^{-3}. These data have also been analyzed assuming the emission measure of a region is described by a two parameter function which decreases exponentially with temperature. Values of the two parameters for the active regions and the general corona will be presented along with implications of these results. Parameters in a theory first proposed by Gabriel and Jordan (1969, MNRAS 151, 141) have been evaluated by this experiment and will also be presented. This work was supported by NASA under Contracts NASw-1834 and NAS2-6723, and by the Lockheed Independent Research Program.

Reference: Bulletin of the Am. Astron. Soc., 4, 379 (1972).